OXIDATIVE-STRESS INDUCED BDNF TRANSPORT DEFICITS

INVESTIGATING MECHANISMS OF OXIDATIVE-STRESS INDUCED BDNF AXONAL TRANSPORT DEFICITS IN BASAL FOREBRAIN CHOLINERGIC NEURONS

By CLAIRE GAGE, B.Sc. Hons.

A Thesis Submitted to the School of Graduate Studies in Partial Fulfillment of the Requirements for the Degree Master of Science

McMaster University

DESCRIPTIVE NOTE

McMaster University MASTER OF SCIENCE (2023) Hamilton, Ontario (Neuroscience Graduate Program)

TITLE: Investigating mechanisms of oxidative-stress induced BDNF axonal transport deficits in basal forebrain cholinergic neurons

AUTHOR: Claire Gage, B.Sc. Hons. (University of Guelph)

SUPERVISOR: Professor Margaret Fahnestock

NUMBER OF PAGES: xv, 61

LAY ABSTRACT

Aging and Alzheimer's disease (AD) involve impairments to the thinking and memory of individuals. This is linked to the degeneration of brain areas such as the basal forebrain, which depends on transport of the protein brain-derived neurotrophic factor (BDNF) from connecting brain regions. A major contributing factor to aging and AD is oxidative stress, which produces harmful molecules that damage cells. This study initially aimed to study if oxidative stress reduces BDNF transport, with the intention of assessing the mechanism behind this effect. The findings of this study showed that while oxidative stress does indeed reduce BDNF transport, it however has no effect on the BDNF receptors or two of the proteins involved in transport, BICD1 and Hook1. Future directions of this work could potentially explore the effect of oxidative stress on other proteins, like htt and DISC1, which are also involved in BDNF transport.

ABSTRACT

Aging and Alzheimer's disease (AD) are associated with decreased cognitive function and neural degeneration. The basal forebrain is one of the first areas of the brain to degenerate in AD and depends on the neurotrophin brain-derived neurotrophic factor (BDNF) for survival. Loss of BDNF transport from target neurons may contribute to basal forebrain cholinergic neuron (BFCN) vulnerability in AD and aging. Oxidative stress is associated with cholinergic dysfunction and cognitive decline in aging and AD, and it is possible that oxidative stress may contribute to BDNF transport deficits in BFCNs. BFCNs are grown in microfluidic chambers that allow isolation of BFCN soma and axon terminals so transport of biotinylated and fluorescently labelled BDNF can be quantified.

The objective of my research was to determine if oxidative stress induces BDNF retrograde transport deficits in BFCNs, and the mechanism behind this effect. I found that oxidative stress does reduce BDNF retrograde transport in BFCNs. Because it has previously been shown that aged BFCNs have decreased BDNF transport and downregulate the BDNF receptor TrkB, expression of both TrkB and $p75^{NTR}$ receptors was tested following oxidative stress using immunocytochemistry (ICC) and western blotting. This experiment showed that oxidative stress does not affect $p75^{NTR}$ or TrkB receptor levels. A likely alternative is that oxidative stress may lead to alterations in the transport machinery responsible for retrograde BDNF transport.

I hypothesized that oxidative stress decreases retrograde axonal transport of BDNF via increased insulin-like growth factor 1 receptor (IGF1R) activity, which decreases the protein expression of the adaptor proteins BICD1 and Hook1 by inhibiting GSK3β activity via the PI3K-

Akt pathway. ICC and western blotting showed that oxidative stress has no effect on either BICD1 or Hook1 levels.

Future directions of this work involve further studying the involvement of the IGF1R pathway in oxidative stress, and the effect on other proteins involved in BDNF transport, including htt and DISC1.

ACKOWLEDGEMENTS

I would like to begin by expressing my gratitude to my supervisor, Dr. Margaret Fahnestock. Working under her guidance in her lab has been an extraordinary opportunity. The experiences I've gained and the knowledge I've acquired during this time have been instrumental in shaping me as a scientist. Dr. Fahnestock's support and mentorship have been crucial in helping me develop a wide range of invaluable skills.

I am also immensely thankful to my committee members, Dr. Angela Scott and Dr. Judith West-Mays. Their profound expertise in molecular biology played a pivotal role in advancing my research. Their insights and feedback were invaluable throughout my academic journey.

A special mention goes to my lab mates, whose camaraderie and assistance have been indispensable. Crystal Mahadeo, Erika Kropf, Mona Abdolahi, and Sama Jaberi, you have been a great support to me. Crystal, Erika, and Mona, thank you for patiently training me in the experimental techniques essential for my project. I also thank our lab technician, Bernadeta Michalski, whose guidance and endless advice significantly enriched my research. Bernadeta was always available to discuss results and suggest new ideas, for which I am truly grateful.

Thank you to all the undergraduate students who contributed their effort to the lab: Aishwaria Maxwell, Anish Puri, Elise Chiu, Helena Son, Shiyani Balakumar, Bosong Wang, Leanna D'Souza, and Sai Pasumarthi. Your dedication to research and support in the lab was indispensable to all of us.

My heartfelt appreciation extends to the friends who provided unwavering mental support along this challenging journey. Lastly, and most importantly, I want to express my profound gratitude to my family. Their continuous love and unwavering support have been my anchor throughout these two years. Without them, this accomplishment would not have been possible.

Thank you all for being an essential part of my academic and personal growth.

TABLE OF CONTENTS

LIST OF FIGURES

LIST OF TABLES

LIST OF ABBREVIATIONS

AD	Alzheimer's Disease
Akt	Protein kinase B
AOD	Antioxidant deprivation
Aβ	Amyloid beta
BDNF	Brain-derived neurotrophic factor
BFCN	Basal forebrain cholinergic neuron
BICD1	Bicaudal D homolog 1
BirA	Biotin ligase
BSA	Bovine serum albumin
CaN	Calcineurin
DAPI	4′,6-diamidino-2-phenylindole
DISC1	Disrupted in schizophrenia 1
ERK	Extracellular signal-regulated kinase
ETC	Electron transport chain
FBS	Fetal bovine serum
GSK3β	Glycogen synthase kinase 3 beta
HAP1	Huntingtin-associated protein 1

HD	Huntington's Disease
Hook1	Hook microtubule tethering protein 1
Htt	Huntingtin
ICC	Immunocytochemistry
IGF1R	Insulin-like growth factor receptor 1
JNK	c-Jun N-terminal kinase
LTD	Long-term depression
LTP	Long-term potentiation
$p75^{NTR}$	Pan-neurotrophin receptor
PBS	Phosphate buffered saline
Pen Strep	Penicillin Streptomycin
PI3K	Phosphoinositide 3-kinase
PLCγ	Phospholipase C gamma
PLL	Poly-L-lysine
PMSF	Phenylmethylsulfonyl fluoride
PPP	Picropodophyllotoxin
QD	Quantum dot
ROS	Reactive oxygen species

SEM	Standard error of the mean
TBS	Tris buffered saline
TF	Transcription factor
TrkB	Tropomyosin receptor kinase B
TrkB.FL	Full-length TrkB
TrkB-Shc	Sarc homology containing TrkB
TrkB.T1	Truncated TrkB
YFP	Yellow fluorescent protein

DECLARATION OF ACADEMIC ACHIEVEMENT

I performed all experimental procedures including cell culture, transport assays, immunocytochemistry, and western blotting.

SECTION 1: INTRODUCTION

1.1 Aging and Alzheimer's Disease

The aging population in Canada has drastically increased in recent years and is expected to triple in the next 25 years.[1] With this increase in older adults will be an increase in age-related diseases. Normal aging can cause decreases in certain cognitive abilities, such as working memory, attention, declarative memory, and executive function.[2] This is accompanied by changes to the brain including decreases in grey matter volume, number of neurons, and synaptic density in regions important for cognitive function such as the cortex, hippocampus, and basal forebrain.[2,3] However, when an individual experiences significant changes to cognitive ability and daily function, they may be experiencing mild cognitive impairment or dementia. Alzheimer's disease (AD) is the most common form of dementia, currently affecting close to 600,000 individuals in Canada, which is expected to increase to nearly 100,000 by 2030.[4] AD is a devastating neurodegenerative disease that causes progressive loss of memory and cognitive function, usually affecting older adults, as the greatest risk factor for AD is age.[5]

A pathological characteristic of all neurodegenerative diseases is the accumulation of abnormally folded protein aggregates.[6] In AD, there are two types of fibrillar protein aggregates that form in the affected areas; extracellular amyloid plaques consisting of amyloid-beta proteins, and intracellular neurofibrillary tangles consisting of hyperphosphorylated tau protein.[7] Amyloid plaques form when amyloid precursor protein, a cell membrane protein, is processed and cleaved to form Aβ protein, which aggregates and forms plaques between cells.[7] Tau is a microtubule associated protein which normally interacts with α and β tubulin proteins to promote and stabilize axonal microtubule formation.[8] Microtubules are part of the cell cytoskeleton and are

important for maintaining cell structure and intracellular transport. The natural tau protein is an unfolded, soluble protein with little secondary or tertiary structure. But post-translational modifications such as phosphorylation, truncation, and acetylation can cause tau to gain secondary structures.[8] Phosphorylation is important in regulating the binding of tau to microtubules, and altered phosphorylation states can affect microtubule dynamics.[9] When tau is hyperphosphorylated at key phospho-epitopes, it disrupts microtubule binding, and tau dissociates from the microtubules. It goes through conformational changes and begins to aggregate into oligomers, which can form insoluble paired helical filaments – and these make up the neurofibrillary tangles (NFT) that are found in AD.[10] It was originally believed that NFTs were responsible for degeneration in AD, but soluble tau oligomers actually correlate better than NFTs with cellular and behavioural changes.[11,12] While Aβ and tau pathology are the hallmark lesions associated with AD, there are many other components of AD pathology that contribute to neural degeneration and the development of clinical symptoms. To have a better understanding of the disease, there should be a focus on other factors that contribute to the molecular pathology of neural degeneration, including neurotrophic support and oxidative stress.

1.2 Oxidative Stress

Oxidative stress is caused by an imbalance in the production and clearance of reactive oxygen species (ROS) generated from oxygen metabolism. The main source of ROS is the electron transport chain (ETC) in mitochondria where energy metabolism occurs – free electrons from the ETC leak out and react with oxygen molecules, producing superoxide anions.[13] ROS are free radicals containing an unpaired electron, and superoxide is the precursor to other ROS including hydrogen peroxide, hydroxide, and hydroxyl.[14] ROS have regular functions in the cell at low levels, involving phagocytic destruction of bacteria, cellular signaling, and homeostasis.[15]

But overproduction and accumulation of ROS leading to oxidative stress causes cellular dysfunction and damage. High amounts of ROS in the cell can cause damage to lipid, protein, and DNA structure.[15] ROS can oxidise proteins, make site-specific amino acid alterations, cleave peptide-peptide bonds, and cause the aggregation of proteins. These structural changes can impair the function of proteins, so they must be proteolytically processed and removed to prevent negative interactions with other molecules.[16] ROS are directly involved in cellular aging and death and can affect protein kinase signaling, including activating Akt signaling.[17] Normally, endogenous and dietary antioxidants such as glutathione, Vitamin E, Vitamin C, and superoxide dismutase 1 scavenge ROS and stabilize them by donating electrons to reduce them.[15] However, in cases of oxidative stress there is more production than clearance of ROS. Increased oxidative stress occurs during normal aging, and even more so in AD.[16]

Oxidative damage and deficits in the antioxidant system are associated with the cholinergic dysfunction and cognitive decline seen in aging and AD[18]. Animal models have shown that oxidative stress begins before the development of other AD pathology,[18] and post-mortem AD patients' brains have been found to contain oxidized molecules.[19] It is believed that there may be a cycle whereby aging and AD pathology, including aggregated Aβ and tau, may enhance free-radical production and reduce the clearance of oxidized proteins, and oxidative stress may also contribute to early cellular pathological occurrences.[15,20,21]

1.3 Brain-Derived Neurotrophic Factor

Neurotrophins are a family of proteins found in the brain which are important for the survival and function of neurons. Brain-derived neurotrophic factor (BDNF) is one neurotrophin which plays an important role in learning and memory. Decreased BDNF expression is correlated with cognitive impairment in AD, while exogenous BDNF administration rescues cognitive

impairment in AD mouse models.[22,23] There are three forms of BDNF that exist in the brain; the immature pro-BDNF protein can be cleaved by proteases into the mature BDNF protein, or cleaved by different enzymes to form a truncated BDNF species. BDNF can activate two receptors: the pan-neurotrophin receptor ($p75^{NTR}$) and tropomyosin receptor kinase B (TrkB). Pro-BDNF mainly binds $p75^{NTR}$ while mature BDNF mainly binds TrkB, and they each activate different signaling pathways (Figure 1).

TrkB has three main isoforms, TrkB full-length (TrkB.FL) and two truncated forms (TrkB.T1 and TrkB-Shc).[24] When BDNF binds TrkB, the receptor is autophosphorylated and recruits adaptor proteins which aid in activating three signaling pathways. These include the phospholipase-Cγ (PLCγ) calcium pathway, phosphatidylinositol 3 kinase (PI3K) protein kinase B (Akt) pathway, and the mitogen-activated protein kinase (MAPK)/ extracellular signal-regulated kinase (ERK) pathway.[25] These pathways are all involved in promoting long-term potentiation (LTP) and synaptic plasticity, neuronal survival, cell differentiation, and neurite outgrowth.[26] When BDNF binds to $p75^{NTR}$ with its co-receptor sortilin, it signals apoptosis and regulates synaptic connections by long term depression, through the activation of c-Jun N-terminal kinase (JNK)/caspase-3.[27]

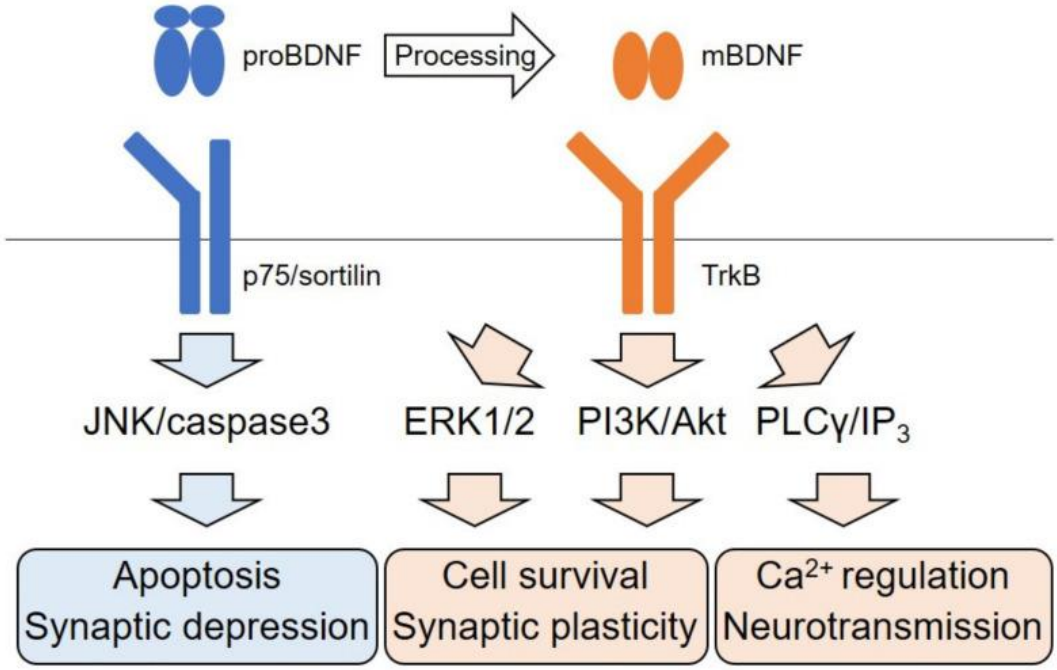

Figure 1: BDNF signaling through $p75^{NTR}$ and TrkB receptor activation.

proBDNF promotes apoptosis and weakens synaptic connections by binding to $p75^{NTR}$ and sortilin receptor complex, activating JNK/caspase-3 signaling pathways. When BDNF is cleaved to the mature form, it binds to TrkB and activates signaling pathways that promote cell survival, LTP, and cell differentiation (adapted from Numakawa & Odaka, 2021).[28]

1.4 The Basal Forebrain

The basal forebrain is a region of the brain that is important for learning and memory and is made up of a collection of nuclei that project their axons throughout the cortex and hippocampus. The basal forebrain is one of the first areas of the brain to degenerate in AD,[29] and synaptic loss of basal forebrain cholinergic neurons (BFCNs) correlates with cognitive decline.[30] BFCNs are dependent on neurotrophic factors such as BDNF for survival and function.[31] BDNF is highly expressed in the hippocampus and cortex but is not expressed by BFCNs. To obtain BDNF, BFCNs must retrogradely transport it from target neurons.

Axonal degeneration occurs early in AD, and is also seen in animal models.[32] It precedes neuronal cell death, and understanding the mechanism of retrograde transport is important to prevent loss of neurons and cognitive function. In AD, neurons undergo a process called 'dying back degeneration', which begins with dysfunction of synaptic connection, followed by degeneration of axons in a distal-to-proximal direction, and one of its molecular causes is believed to be disrupted axonal transport.[32] Studies have shown that disruptions in axonal transport are sufficient to cause degeneration of neurons,[33] so loss of BDNF transport may contribute to BFCN vulnerability in AD and aging. BDNF retrograde axonal transport and TrkB protein expression are reduced in rat BFCNs with age[34], but the mechanism by which this occurs is unknown.

The basal forebrain has been shown to be particularly sensitive to oxidative damage due to its high metabolic demand. [35] In a Down's Syndrome model, oxidative stress was found to contribute to BFCN degeneration and cognitive decline, and antioxidant treatment delayed these pathologies.[36] It is possible that oxidative stress may contribute to BDNF transport deficits in BFCNs. However, the underlying mechanism of this effect remains to be elucidated.

1.5 Transport Mechanics of BDNF

Once BDNF is bound to its receptor at axon terminals, it can activate its associated signaling pathways in the axon terminal or be transported to the cell body (summarized in Figure 2). BFCNs have very long axonal projections, so it is very important for BDNF to be properly transported all the way from target neurons. After BDNF binds to a receptor, the protein and receptor complex goes through clathrin-dependent endocytosis into a signaling endosome that is transported along microtubules by motor proteins.[37]

In general, signaling endosomes can be transported either from the cell body towards the axon terminal, in the anterograde direction, or from axon terminals towards the cell body, in the retrograde direction. There is different machinery responsible for both directions of movement. Kinesins are responsible for anterograde transport, while dynein is responsible for retrograde transport. Dynein forms a motor complex with dynactin, and together both are necessary for retrograde transport of cargo.[38]

There are many adaptor proteins involved in BDNF/TrkB endosome transport. Huntingtin protein (htt) is an adaptor between endosomes and dynein. Huntingtin-associated protein 1 (HAP1) aids in BDNF endocytosis and tethers signaling endosomes to microtubules by connecting htt with BDNF vesicles and a component of dynactin, p150Glued.[39–41] When htt forms this complex, it controls the direction of movement of BDNF, depending on the phosphorylation state of htt.[42] When the S421 site is phosphorylated, htt binds to kinesin promoting anterograde transport, and when it is dephosphorylated, it releases kinesin and allows htt to bind dynein for retrograde transport.[43] Htt can be phosphorylated by Akt, and it can also be controlled by calcium signaling. When BDNF binds to TrkB, PLCγ is activated and initiates an influx of calcium,[44] which activates calcineurin (CaN). CaN then dephosphorylates htt S421,

activating retrograde transport.[39] Rab GTPases are also involved in BDNF transport. Rab5 and Rab7 help regulate BDNF transport along microtubules by recruiting the dynein-dynactin motor complex and promoting vesicle formation.[45,46]

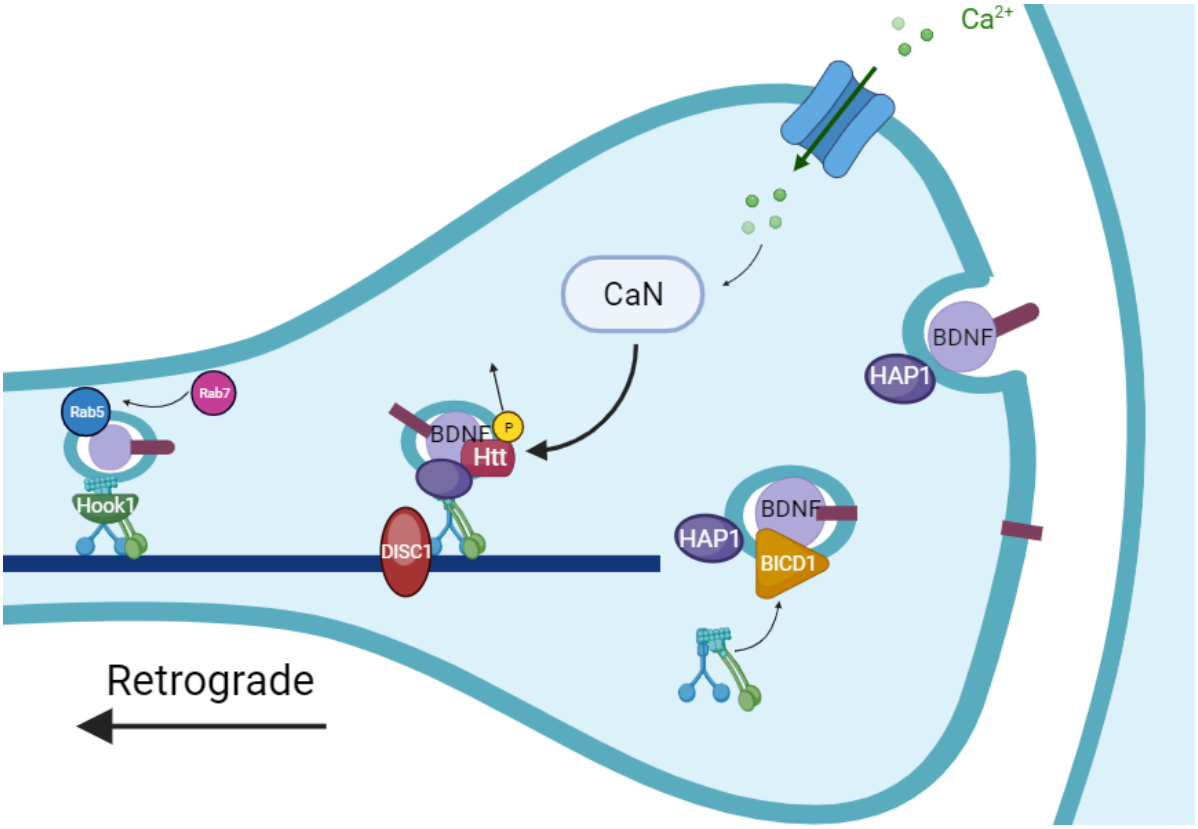

Figure 2: Proteins involved in retrograde BDNF transport.

Many adaptor proteins help regulate the transport of BDNF. Rab5 and HAP1 help with vesicle formation and recruitment of dynein to the vesicle. In the late-endosome, Rab5 is converted to Rab7, which helps regulate transport to late endocytic compartments. Htt binds to HAP1, and controls the direction of vesicle movement based on its phosphorylation state. Calcium influx caused by TrkB signaling activates CaN, which dephosphorylates htt promoting retrograde movement. DISC1 helps associate dynein and stabilize microtubules. Hook1 stabilizes the interaction between dynein and dynactin. BICD1 also aids in recruiting the dynein-dynactin complex (created with BioRender.com).

1.6 Insulin-like Growth Factor 1 Receptor

Insulin-like growth factor 1 receptor (IGF1R) is a growth hormone receptor found in many tissue types in the body, including the CNS. IGF1R signaling is involved in growth and metabolism, and in the brain it is important for development and plasticity.[47] Recently, it has been implicated in AD pathology, and inhibiting IGF1R signaling has been found to decrease soluble Aβ levels,[48] increase synaptic density, reduce oxidative damage, and improve cognitive function.[49] IGF1R can also be activated by reactive oxygen species – there is evidence for "cross talk" between IGF1R and ROS signaling.[50] One study found that heterozygous knock-out of IGF1R in mice increased their lifespan and resistance to oxidative stress.[51] It is possible that increased IGF1R signaling caused by oxidative stress may also contribute to the degeneration of the basal forebrain in AD and aging.

In particular, inhibiting IGF1R signaling increases the speed of BDNF-containing endosome retrograde transport in motor neurons.[52] This was tested in signaling endosomes transporting a binding fragment of tetanus toxin, which is known to colocalize with BDNF/TrkB in signaling endosomes.[53,54] IGF1R inhibition does not affect mitochondrial or lysosomal transport, indicating that IGF1R does not modulate cytoplasmic dynein directly.[52] IGF1R inhibition decreases Akt activity, and IGF1 is known to activate the PI3K/Akt pathway. Akt inhibition increases BDNF endosome transport speed, suggesting that this pathway influences axonal transport.[52]

Further, evidence shows that IGF1R inhibition increases Bicaudal D homolog 1 (BICD1) protein expression.[52] BICD1 is a dynein motor adaptor protein which is known to regulate TrkB and $p75^{NTR}$ trafficking and sorting[55] and to recruit the dynein complex to promote retrograde transport of organelles in mammalian neuronal cells.[56] It has been suggested that altering levels

of BICD1 protein expression may be the mechanism by which IGF1R regulates BDNF endosome retrograde transport.[52] It is also known that Akt activation phosphorylates GSK3β (Ser9), inhibiting GSK3β activity.[57,58] Hypoxia – a state which produces oxidative stress – has been shown to regulate the interaction of BICD1 and its binding proteins via Akt/GSK3β.[59] GSK3β has been shown to stabilize the interaction of BICD1 with dynein through BICD1 phosphorylation.[60] IGF1R may reduce BDNF endosomal transport speed via decreased BICD1 protein expression and reduced interaction between BICD1 and dynein through the Akt/GSK3β pathway.

GSK3β can also control protein expression through regulation of transcription. It can phosphorylate many transcription factors (TF), which then bind to the promoter region of DNA to regulate the rate of transcription of specific genes. It can also regulate gene expression through direct phosphorylation of histones, histone deacetylases, and histone acetyltransferases. Hook1 is another dynein adaptor protein which is necessary for retrograde transport of BDNF/TrkB signaling endosomes, as depletion of Hook1 decreases BDNF/TrkB transport.[61] Hook1 interacts with dynein and dynactin, stabilizing their interaction to form a motor complex necessary for BDNF/TrkB transport. One study showed that GSK3β inhibition downregulates Hook1 gene expression in differentiated induced pluripotent stem cells.[62] It is therefore possible that Hook1 expression could also be inhibited by aberrant IGF1R signaling via GSK3β inhibition,[63] reducing BDNF retrograde transport. Hook1 protein expression is decreased in the AD brain,[64] and this may be caused by oxidative stress and IGF1R signaling.

SECTION 2: OBJECTIVES AND HYPOTHESIS

The overall objective of my research is to determine the mechanism of oxidative-stress induced BDNF retrograde transport deficits in BFCNs.

2.1 Objective 1: Determine if oxidative stress affects retrograde axonal transport of BDNF in BFCNs.

I hypothesized that oxidative stress causes a decrease in BDNF retrograde transport in BFCNs.

2.2 Objective 2: Determine if oxidative stress affects neurotrophin receptor expression.

I hypothesized that oxidative stress has no effect on $p75^{NTR}$ protein expression, but TrkB expression is decreased by oxidative stress.

2.3 Objective 3: Determine if oxidative stress affects Hook1 or BICD1 protein expression in BFCNs.

I hypothesized that oxidative stress decreases retrograde axonal transport of BDNF via increased IGF1R activity, which decreases protein expression of BICD1 and Hook1 by inhibiting GSK3β activity through the PI3K-Akt pathway (Figure 3).

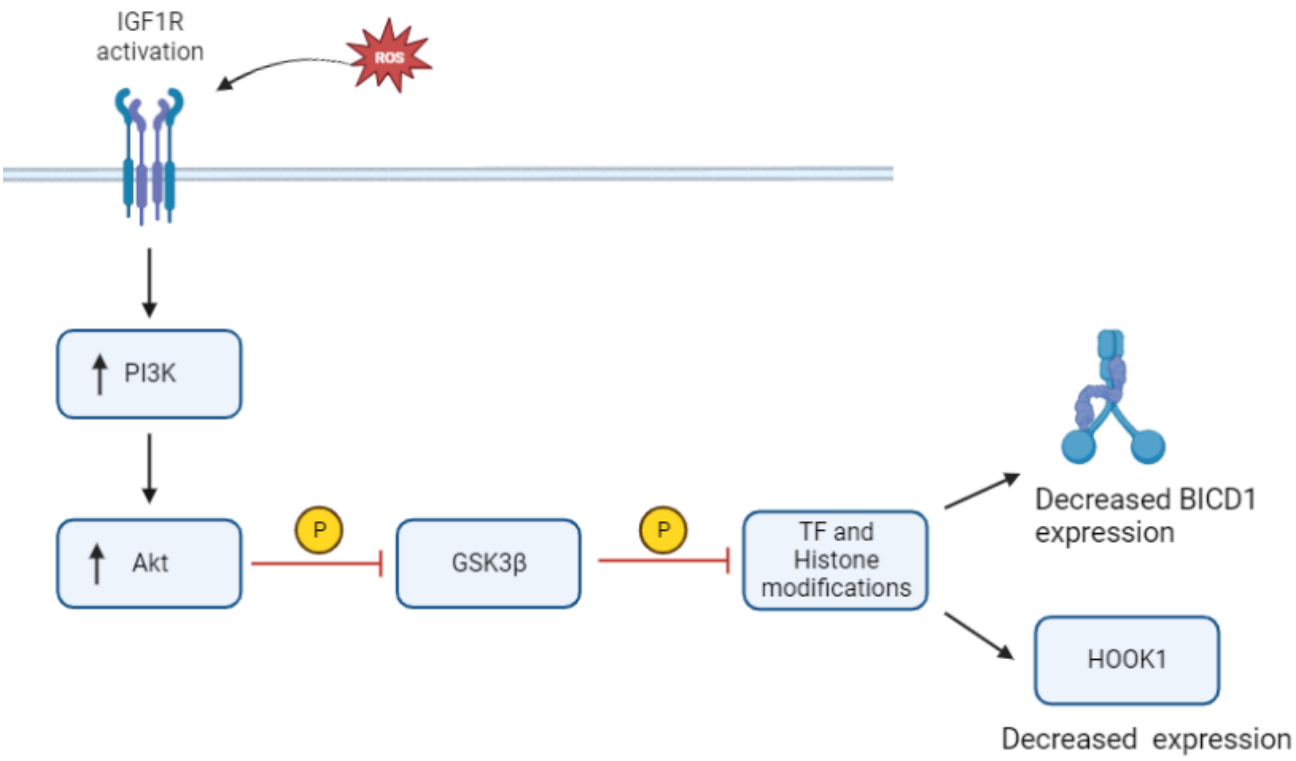

Figure 3: Hypothesized mechanism of oxidative-stress induced BDNF transport deficits.

I hypothesized that oxidative stress decreases retrograde axonal transport of BDNF via increased IGF1R activity, which decreases protein expression of BICD1 and Hook1 by inhibiting GSK3β activity through the PI3K-Akt pathway (created with BioRender.com).

SECTION 3: METHODOLOGY

3.1 Primary Cell Culture and Treatment

The day before dissection, microfluidic chambers (Xona Microfluidics, Temecula CA, cat#XC450) were prepared following the protocol provided by the manufacturer. 95% ethanol was added to each well and subsequently rinsed twice with phosphate buffered saline (PBS; 137 mM sodium chloride, 2.7 mM potassium chloride, 0.9 mM potassium phosphate, 6.4 mM sodium phosphate, 7.4 pH). Poly-L-lysine (PLL; Sigma Aldrich, St. Louis MO, cat#P4707) was then added to each well and the chambers were left to incubate overnight at 37°C, 5% CO2. The next day, each well was rinsed with PBS. Plating medium consisting of Neurobasal (Thermo Fisher Scientific, Burlington ON, cat#21103-049), 1% Penicillin-Streptomycin (Pen Strep), 1X B-27 supplement (Thermo Fisher Scientific, cat#17504-044), 1X GlutaMAX supplement, 1% FBS, 50ng/mL BDNF (Peprotech, Rocky Hill NJ), and 50 ng/mL NGF (generously provided by Dr. Michael Coughlin, McMaster University, Hamilton ON) was then added to each well. The chambers were incubated at 37°C, 5% CO2 throughout the course of the dissection. The basal forebrain was dissected from embryonic day 18 (E18) Sprague-Dawley rat and B61295F2/J mouse embryos and stored on ice in Hank's Balanced Salt Solution (HBSS; Thermo Fisher Scientific, cat#14185-052) with 1% Pen Strep. The basal forebrains from all embryos (3-8) were pooled and washed five times with fresh HBSS. 0.5% trypsin-EDTA (Thermo Fisher Scientific, cat#15400-054) was diluted to 0.025% in HBSS, and the tissue was incubated in a 37°C water bath for 20 minutes, gently shaking every 5 minutes. Following the 20-minute digestion, DNAse I (Sigma Aldrich, cat#10104159001) was added to a final concentration of 1mg/mL. The tissue was then mechanically digested via trituration with a sterile glass pipette. 1 ml of plating medium was immediately added, and the tissue was centrifuged at 448 x g at room temperature for 4

minutes. The pellet was then resuspended in 66.7 µl of plating medium per embryo dissected. The cells were then counted using a hemocytometer.

For microfluidic chambers, after removing the medium from all wells of the chambers, an amount of the cell solution needed for a density of 125,000 cells/well was added to each well on the cell body side of the chambers. Cells were incubated at 37°C, 5% CO2 for 5 minutes to allow the cells to adhere, and then 150 µl of plating media was added to each well. For protein harvest, cells were seeded at a density of 1 x 10 cells/well in 6-well plates (Sarstedt, Newton NA, cat#83.3920.005). For immunocytochemistry experiments, cells were seeded at a density of 40,000 cells/well in Nunc 96-well optical-bottom plates (Thermo Fisher Scientific, cat#265300). Cells were then incubated overnight at 37°C, 5% CO2. The following morning, the plating media was removed and replaced with serum-free maintenance medium (Neurobasal, 1% Pen Strep, 1X B-27 supplement, 1X GlutaMAX supplement, 50ng/mL BDNF, and 50 ng/mL NGF). The cell medium was changed every 48-72 hours prior to cell treatment.

Oxidative stress was produced by culturing BFCNs in antioxidant-free medium for 24h. This medium was the same as maintenance medium except it used B-27 supplement minus antioxidants (Thermo Fisher Scientific, cat#10889038), which lacks the antioxidants vitamin E, vitamin E acetate, superoxide dismutase, catalase, and glutathione. It has previously been shown that 24h antioxidant deprivation with this medium induces oxidative stress in BFCNs *in vitro* (Figure 4).[65] The antioxidant deprivation treatment causes a significant increase in CellROX fluorescence, meaning an increase in ROS in the cells, which is an indicator of oxidative stress.[66,67] CellROX fluorescence colocalized with MitoSOX, an indicator of mitochondrial superoxide, demonstrating that there is an increase in production/reduction of clearance of ROS produced from cellular respiration.

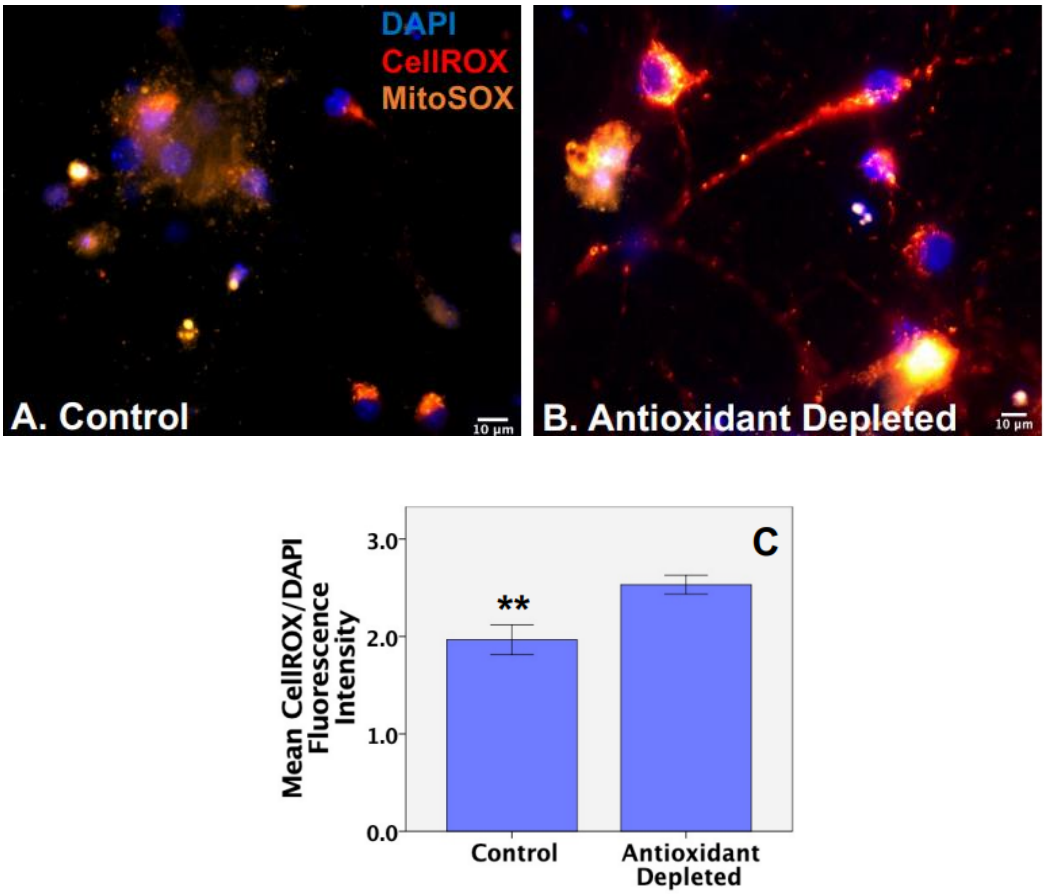

Figure 4: 24h antioxidant deprivation causes oxidative stress in BFCNs.

BFCNs demonstrate significantly increased CellROX fluorescence, indicative of ROS accumulation, after being cultured in antioxidant poor medium for 24 hours (A-C). CellROX fluorescence colocalized with mitochondrial superoxide indicator MitoSOX following antioxidant deprivation (B). N= 40 images, error bars indicate SEM. **p= 0.007 (adapted from Shekari, PhD Thesis).[65]

3.2 Neurotrophin Production

A pcDNA 3.1 expression vector containing a pre-proBDNF sequence, a biotin-accepting AVI region, and a 6xHis tag for Ni purification was generously provided by Dr. Chengbiao Wu, USCD. 16 µg of this plasmid was co-transfected with an equal amount of a plasmid coding for biotin ligase (BirA) (provided by Dr. Chengbiao Wu, USCD) into HEK293FT cells. Cells were grown in a 10cm petri dish in medium composed of Dulbecco's modified eagle medium (DMEM; Thermo Fisher Scientific, cat#12800-082), 1% Fetal bovine serum (FBS; Thermo Fisher Scientific, cat#12483-020), 1% Pen Strep (Thermo Fisher Scientific, cat#15140-122), 200mM GlutaMAX supplement (Thermo Fisher Scientific, cat#35050-061), and 100mM sodium pyruvate (Sigma Aldrich, cat#S8636) until they reached 70% confluency. 24 hours before transfection, the medium was changed to a serum-free medium, identical to the growth medium but lacking FBS, and with the addition of 50uM D-biotin (Sigma Aldrich, cat#58-85-5). To make both BirA and BDNF transfection mixtures, 16 µg of DNA was added to 1mL of DMEM with 60 µL of TurboFect Transfection Reagent^{TM} (Thermo Fisher Scientific, cat#R0531). These were mixed by inverting and left at room temperature for 15 min. The transfection mixtures were both added to the Petri dish dropwise and incubated at 37°C, 5% CO2 for 72 hours.

After transfection, nickel affinity chromatography was used to purify BDNF-biotin from the medium. The supernatant was removed from the cells and centrifuged for 10 min at 9660 x g at 4 ºC. 1.2mL of HisPur Ni-NTA Resin (Thermo Fisher Scientific, cat#88221) was centrifuged briefly, the liquid was removed from the top, then 900 µL wash buffer was added (30mM PBS, 500mM NaCl, 20mM imidazole, 1mM phenylmethylsulfonyl fluoride (PMSF). The supernatant from the cell medium was added to 30 mL wash buffer and the prepared Ni-NTA. This was stirred overnight at 4 ºC. The following day, a 5.0 × 20 cm chromatography column (Bio-Rad,

Hercules CA, cat#7375021) was wet with wash buffer, then the protein+Ni mixture was added to the column. When the protein had mostly run through the column into a flask, the flow-through was added back to the column. When this had almost fully run through the column, 30mL elution buffer (30mM PBS, 500mM NaCl, 300mM imidazole, 1mM PMSF) was added and the flow-through collected. The protein was concentrated using Amicon Ultra centrifugal filters (Sigma Aldrich, cat#UFC901024). 15 mL of the protein in elution buffer was added to each concentrator and spun at 4000 rpm for 10 min. The concentrated protein was aliquoted into 20 µL aliquots and stored at -80 ºC. The concentration of the resulting BDNF protein was determined using the Human/Mouse BDNF DuoSet ELISA kit (R&D Systems, Minneapolis MN, cat#DY248) following the manufacturer's instructions.

3.3 Labelling Neurotrophins

7.76 ng of the biotinylated BDNF protein (20 uL) was incubated in the dark, on ice, for 1 hour with Quantum Dot 625 Streptavidin conjugate (Thermo Fisher Scientific, cat#Q22063) in a 1:1 molar ratio. Following the incubation, the final protein concentration was diluted to 43ng/mL using cell culture medium.

3.4 Axonal Transport Assay

Microfluidic chambers were used to separate neuronal cell bodies from axons. These chambers contain two fluidically isolated channels, one for the cell bodies and one for the axon terminals, which are connected by microgrooves. After the neurons adhere in the cell body channel, their axons grow through the microgrooves and terminate in the axon terminal channel. The fluidic isolation of the cell bodies from the axon terminals allows axonal transport to be analyzed in a direction-specific manner, since labelled neurotrophic factors can be added specifically to the

axon terminals in fluidic isolation from the cell bodies (Figure 5). The only way for these factors to reach the cell bodies is to travel along the axons through the microgrooves.

Axonal transport was quantified by imaging the quantum-dot labelled neurotrophins described above by epifluorescence fluorescence microscopy on BFCNs cultured 9 days *in vitro*. BFCN cell bodies and axons were incubated overnight at 37°C, 5% CO2 in maintenance medium lacking BDNF. In the morning, any residual neurotrophin was removed by washing with neurotrophin-free maintenance medium three times. 80µL of medium containing 43ng/mL Quantum dot labelled BDNF was added to the axonal side of the chambers for one hour at 37°C, 5% CO2. At the same time that BDNF was added to the axonal compartment, tubulin was stained with 1 µM Tubulin Tracker Deep Red (Thermo Fisher Scientific, cat#T34077). BFCN nuclei were also stained using NucBlue Live ReadyProbes 34 Reagent (Thermo Fisher Scientific, cat#R37605), 2 drops were added to 1mL wash medium, along with 1 µM Tubulin Tracker Deep Red, then 150 µL of this medium was added to cell body wells.

Following the incubation, the BFCNs were washed with neurotrophin-free maintenance medium three times to remove residual BDNF, then placed in the environmental chamber of the EVOS2 FL microscope, set to 37°C, 5% CO2 to be imaged. The Qdot625 filter was used to image the quantum dots, Tubulin was imaged using the Cy5 filter, and BFCN nuclei were imaged using the 4′,6-diamidino-2-phenylindole (DAPI) filter. ImageJ was used to quantify quantum dot fluorescence at the axon terminals as indications of axonal neurotrophin binding. Tubulin signal was used to select the area of the axons, and QD fluorescence within this area was measured. The QD fluorescence was then normalized to the tubulin fluorescence within the same area. The number of quantum dots was also counted in the proximal axons (imaged at the cell

body end of the microgrooves) as a measure of neurotrophin retrograde transport. The number of QDs present was normalized to total tubulin fluorescence in the proximal axon images.

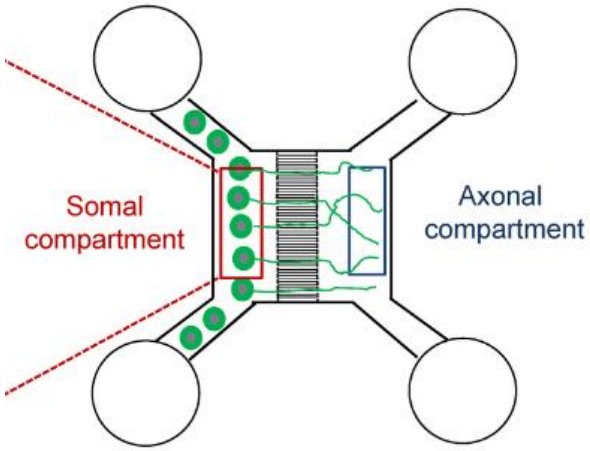

Figure 5: Microfluidic chamber used for axonal transport assays.
Two compartments are fluidically isolated and connected by microgrooves. Cells are plated on one side, and their axons grow across the microgrooves into the opposite compartment, where BDNF is added and transported towards the cell bodies (adapted from Xona Microfluidics).[68]

3.5 Protein Extraction

Cells were harvested on ice from 6-well plates using homogenization buffer containing 50 mM Tris, 10 mM ethylenediamine tetra-acetic acid (EDTA), 0.5% Tween-20, 1X PhosSTOP phosphatase inhibitor cocktail (Roche, Indianapolis IN, catalog#4906837001), and 1X Halt Protease & Phosphatase Inhibitor Cocktail (Thermo Fisher Scientific, catalog #1861284). First, all medium was removed, and cells were washed with 1 mL of cold PBS. All PBS was then removed, 150 µL of homogenization buffer was added to each well and incubated for 10 minutes. Cells were then scraped and collected in 1.5 mL Eppendorf tubes, then sonicated 2X 7

seconds and left on ice for 10 min, then centrifuged at 4˚C and 9660 x g for 20 minutes. The supernatant was removed and put into separate Eppendorf tubes and stored at -80˚C until use.

Protein concentration of the cell supernatants was determined with a detergent compatible (DC) protein assay (Bio-Rad). Protein standards were made using BSA diluted in homogenization buffer. 5 µL of sample supernatant and standards were loaded into a 96 well plate in duplicate. 25 µL of Reagent A (Bio-Rad, cat#5000113) was added, followed by 200 µL of Reagent B (Bio-Rad, cat#5000114). The plate was read after 15 minutes of incubation on a Multiskan Go (Thermo Fisher Scientific), measuring absorbance at 750 nm. Protein concentration of the samples was calculated after creating a standard curve from the known BSA concentrations.

3.6 Western Blot

A 10% polyacrylamide gel was prepared and allowed to polymerize overnight at 4°C. The next morning, samples were prepared by addition of protein lysate, homogenization buffer, and Laemmli Sample buffer (Bio-Rad, catalog #1610747). 900 µL of 4x Laemmli Sample buffer was mixed with 100 µL β-mercaptoethanol. 5 µL of this mixture was added to 15 µg of protein sample, and homogenization buffer was added to a final volume of 20 µL. The sample preparations were briefly centrifuged and boiled for 5 minutes. Condensation was removed from the lid of all tubes by centrifuging for 10 seconds at room temperature. The sample preparations were loaded into the appropriate wells, and the gel was run for 20 minutes at 90V, then at 110V for approximately 1 hour, until the leading dye reached the bottom of the gel.

Samples were then transferred onto a polyvinylidene difluoride (PVDF) membrane (Schleicher & Schuell, Keene NH) in transfer buffer (25mM Tris, 192 mM glycine, 20% methanol) and run at 250 mA using a Bio-Rad PowerPac 300 Electrophoresis power supply,

stirring for 1.5 h at 4°C with an ice pack, which was changed every 30 minutes. Before transfer, the membrane was re-activated by soaking in methanol for 1 minute, then in transfer buffer for 5 minutes on a rocking platform. Sponges and blotting paper were also soaked in transfer buffer on the rocking platform for 5 minutes. Following transfer, the membrane was blocked with 2.5 mL Intercept Protein-Free Blocking Buffer (Li-COR Biosciences, Lincoln Nebraska, catalog #927-80001) and 2.5 mL Tris Buffered Saline (TBS; 20mM Tris, 150mM NaCl), rotating at room temperature for 1 hour. 12µL of 20% Tween-20 and primary antibodies (see Table 1 for dilutions) were then added to the TBS and blocking buffer, and the membrane was left to incubate, rotating overnight, at 4°C. The next morning, the membrane was washed 3x at room temperature with 20-30 ml TBS-Tween for 5 minutes each time. Secondary antibodies (Table 1) were added to 1 mL blocking buffer and 4 mL TBS in a 1:10,000 dilution, and the membrane was left to rotate at room temperature for 1 hour. After the 1-hour incubation, the secondary antibody solution was discarded, and the membrane was washed 3 times at room temperature with 20-30 ml of TBS-Tween for 5 minutes each time. A final wash with 20-30 ml TBS was then completed for 5 minutes at room temperature. The TBS was discarded, and the tube was filled with fresh TBS. The membrane was then scanned with the CDx Odyssey Infrared Imager (Li-COR Biosciences) and analyzed with Image Studio software. Each sample was normalized to its total protein using the Revert 700 Total Protein Stain kit (Li-COR Biosciences, cat#926-11010) following the manufacturer's instructions. Briefly, the membrane was rinsed with ultrapure water, then stained with 10mL of the stain solution for 5 min, gently shaking. Then, the membrane was decanted with the provided wash solution for 30 seconds twice, rinsed again with ultrapure water, and then scanned with the CDx Odyssey Infrared Imager.

3.7 Immunocytochemistry

Immunocytochemistry (ICC) was used to stain for the BDNF receptors TrkB and $p75^{NTR}$ and the motor adaptor proteins BICD1 and Hook1 to test whether there was a decrease in protein expression between AOD treated BFCNs and control BFCNs grown in their usual medium. Briefly, BFCNs grown in optical bottom 96-well plates at a density of 40,000 cells/well were treated with 150 µL/well of AOD or control medium for 24h. Then, BFCNs were rinsed once with 150 µL PBS prior to fixation with 150 µL 4% paraformaldehyde (dissolved in PBS) for 30 minutes at room temperature. BFCNs were again rinsed once with PBS, followed by permeabilization with 0.2% Triton-X100 in PBS for 30 minutes at room temperature.150 µL Blocking solution (3% BSA, 5% FBS, 1% Pen Strep in PBS) was then added for 30 minutes at room temperature. Primary antibodies (see Table 2 for dilutions) were diluted in blocking solution, then 150 µL added to the BFCNs and incubated overnight at 4°C. The next morning, BFCNs were washed 3 times with blocking solution prior to addition of the secondary antibody (Table 2). Secondary antibody was diluted 1:1000 in blocking solution and 150 µL/well was added to the BFCNs for 2 hours at room temperature. BFCNs were then incubated with 150 µL NucBlue Fixed Cell Stain ReadyProbes Reagent (Thermo Fisher Scientific, cat# R37606) diluted 2 drops/mL in PBS for 10 minutes to stain the nuclei, followed by five PBS washes. Finally, BFCN soma were imaged using the EVOS2 FL microscope. The yellow fluorescent protein (YFP) filter was used to visualize the target proteins, and the DAPI filter was used to visualize the stained nuclei. ImageJ was used to quantify the target protein based on fluorescent signal. Background signal was removed from the images using the parameters rolling ball radius: 100 pixels; sliding paraboloid. A Gaussian blur filter was added with a radius (sigma) of 2. To select only the area of the cells, the images were automatically thresholded using the Huang method, to

create a 'mask' of the image. The mask was added to the original image using the image calculator 'multiply' function, and the resulting image was again thresholded, with the minimum value set to 1. Fluorescence was measured as a mean of total fluorescence/area.

3.8 Statistical Analysis

Statistical analysis was performed using GraphPad Prism 9.4.1 software. Data was tested for normality using a Shapiro-Wilk test, followed by either an unpaired t-test, or a Mann-Whitney test if the data were not normally distributed. Outliers were detected using the ROUT method. Power analysis was performed using G*Power3.1 software.

Table 1: Western blotting antibodies

	Antibody	**Dilution**	**Company**
Primary	$p75^{NTR}$	1:1000	Abcam, Waltham MA USA cat#ab227509
	TrkB	1:1000	Cell Signaling Technology, Danvers MA, USA cat#4603S
	BICD1	1:1000	Novus Biologicals, Centennial CO, USA cat#NBP1-85843
	Hook1	1:1000	Novus Biologicals cat#NBP1-81745
Secondary	IR-Dye680 anti-rabbit	1:10,000	LI-COR Biosciences cat#26-68071
	IR-Dye800 anti-rabbit	1:10,000	LI-COR Biosciences cat#926-32211

Table 2: Immunocytochemistry antibodies

	Antibody	Dilution	Company
Primary	$p75^{NTR}$	1:500	Abcam cat#ab227509
	TrkB	1:500	Thermo Fisher Scientific cat#PA578405
	BICD1	1:50	Novus Biologicals cat#NBP1-85843
	Hook1	1:200	Novus Biologicals cat#NBP1-81745
Secondary	AlexaFluor goat anti-rabbit 488	1:1000	Thermo Fisher Scientific cat#A11008

SECTION 4: RESULTS

4.1 Objective 1

4.1.1 Retrograde axonal transport of BDNF is reduced by oxidative stress

An axonal transport assay was used to measure BDNF retrograde transport in BFCNs in conditions of oxidative stress produced by 24h antioxidant deprivation. Measurements of axonal binding of BDNF were normally distributed, so the data were analyzed using an unpaired t-test. No difference in axonal binding of BDNF was seen between AOD and control BFCNs (Figure 6A,B, $p=0.0878$), however there was a trend towards decreased binding in AOD BFCNs. Power analysis showed that a sample size of 131 per group would be needed to reach significance. Significantly fewer BDNF quantum dots were detected at the proximal axons of AOD compared to control BFCNs (Figure 6A,C, $p<0.0001$), meaning there was a reduction in retrograde transport. Both the control ($W=0.8966$, $p=0.0069$) and AOD treated ($W=0.7406$, $p<0.0001$) measurements of proximal axon BDNF were not normally distributed, so the data were analyzed using a Mann-Whitney test.

A

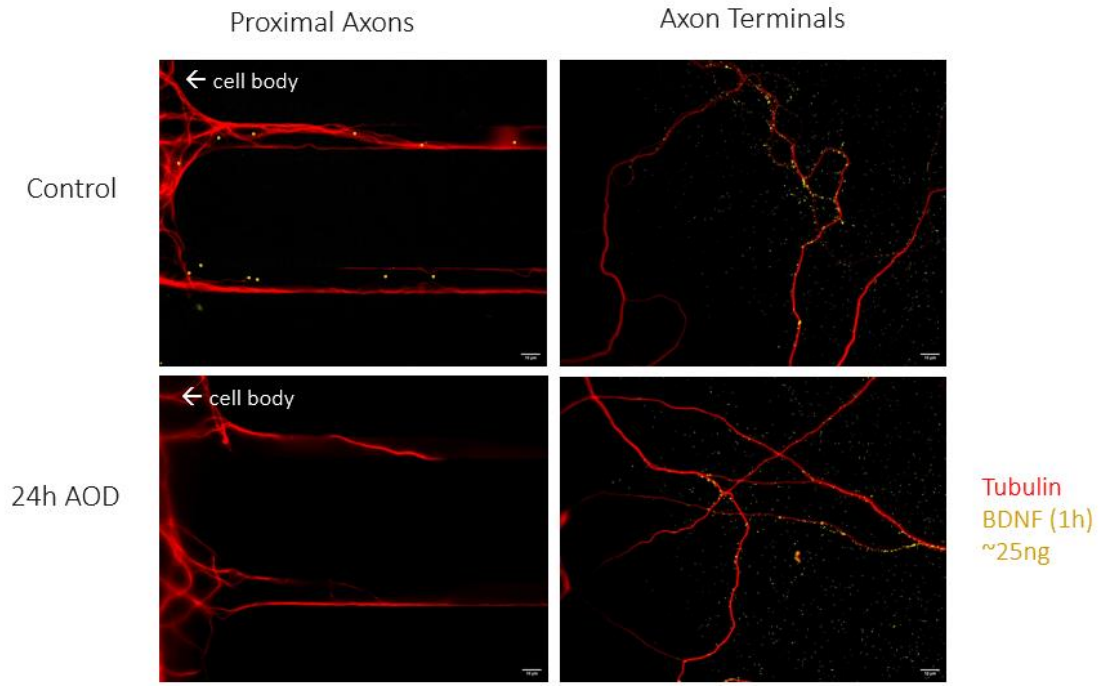
Proximal Axons
Axon Terminals
cell body
cell body
Control
24h AOD
Tubulin
BDNF (1h)
~25ng

B

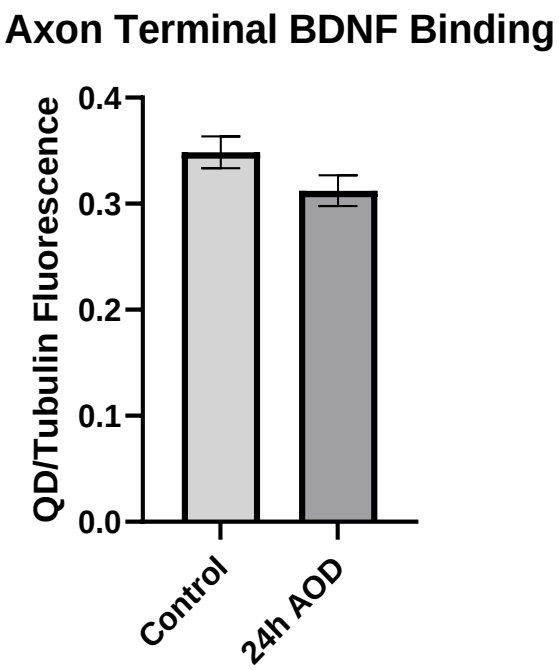
Axon Terminal BDNF Binding
QD/Tubulin Fluorescence
0.4
0.3
0.2
0.1
0.0
Control
24h AOD

C

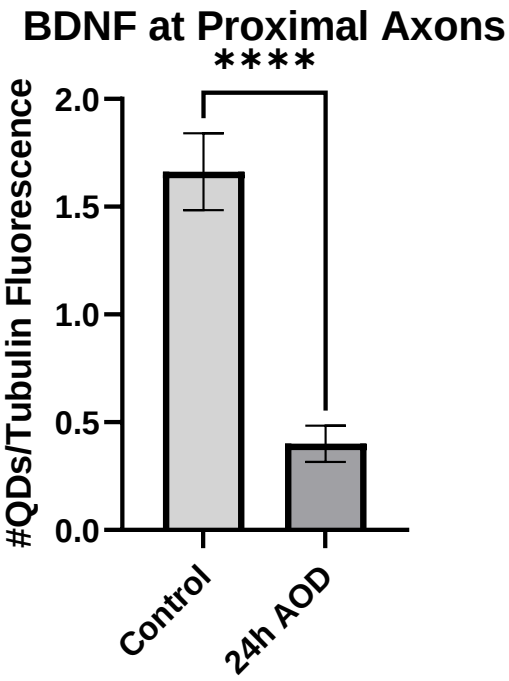
BDNF at Proximal Axons
****
#QDs/Tubulin Fluorescence
2.0
1.5
1.0
0.5
0.0
Control
24h AOD

Figure 6: BDNF retrograde axonal transport is reduced with oxidative stress.

A) Oxidative stress induced by 24h AOD treatment causes decreased transport of BDNF to the proximal axons, and no change in axon terminal BDNF binding. Scale bars are 10 μM. B) Quantification of BDNF binding in axon terminals normalized to tubulin fluorescence, $p=0.0878$. C) Quantification of BDNF at the proximal axons, normalized to tubulin fluorescence, ****$p<0.0001$. N=30 images/group from 3 independent experiments. Error bars represent SEM. Abbreviations: C, control; AOD, antioxidant deprivation; SEM, standard error of the mean; QD, quantum dot.

4.2 Objective 2

4.2.1 Oxidative stress does not affect p75^{NTR} levels

Protein expression levels of p75^{NTR} were tested using ICC and western blotting. For ICC, the data was first tested for normality. Based on a Shapiro-Wilk test, the AOD treated group was normally distributed (W=0.9564, p=0.1262), but the control group did not pass normality (W=0.8823, p=0.0006). Therefore, p75^{NTR} ICC results were analyzed using a Mann-Whitney test. There was no difference in p75^{NTR} levels between control and AOD treated groups (Figure 7, p=0.7832). In western blotting, p75^{NTR} protein was quantified and normalized to the total protein loaded using REVERT total protein stain. There was no significant difference in total protein loaded between control and 24h AOD treated groups (Figure 8A,B, p=0.4). The expected molecular weight of p75^{NTR} is 75 kDa. In the western blot there were two observed bands, at 70.5 kDa and 68 kDa. The 70.5 kDa band is the full-length p75^{NTR} protein, while the 68 kDa band is a truncated isoform lacking exon III, which is formed by mRNA splicing and is missing the extracellular binding domain of the receptor.[69] This truncated isoform lacks the ability to bind BDNF, so only the full-length isoform was analyzed. There was another band present at 81 kDa, but this was non-specific since it also appeared in the p75^{NTR} knockout lysate. Because the same antibody was used for ICC, this means that all proteins detected by the western blot were included in the ICC p75^{NTR} quantification. In Western blotting, when p75^{NTR} was normalized to total protein, based on an unpaired t-test there was no significant difference between 24h AOD treated and control groups (Figure 8A,C, p=0.7342). The n was small, only 3, so power analysis was performed. It was found that a sample size of 246 per group would be needed to reach significance, so the experiment was not replicated.

A

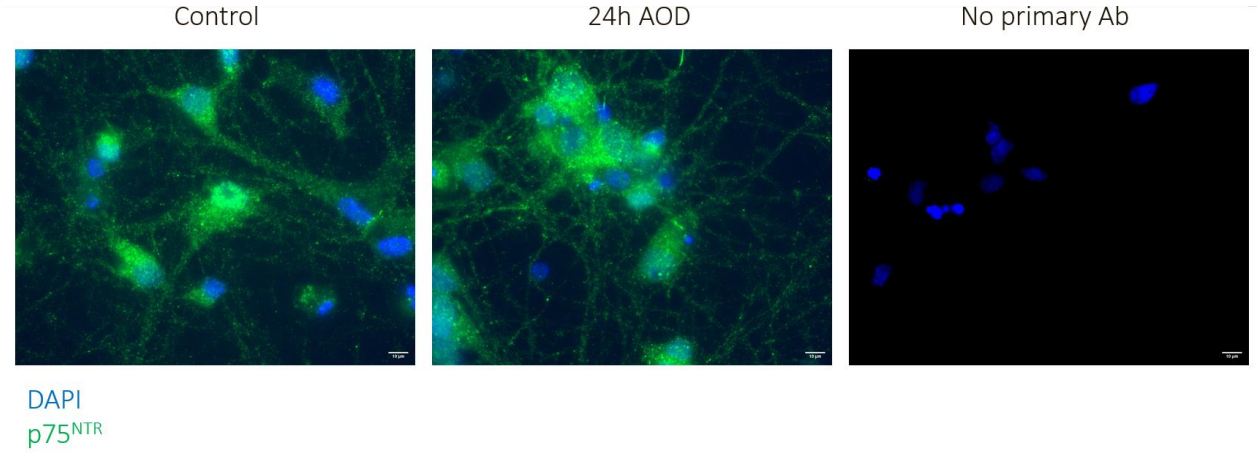

B

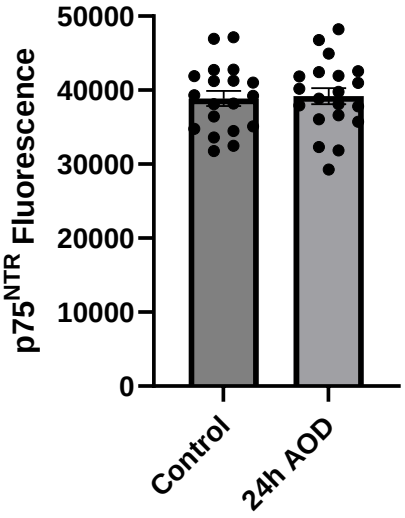

Figure 7: Oxidative stress has no effect on p75^{NTR} expression in BFCNs.

A) When treated with AOD medium for 24h, there was no difference in p75^{NTR} protein levels compared to control medium shown by ICC. A negative control using no primary antibody showed that there was no non-specific binding, indicating that the fluorescent signal was specific to p75^{NTR}. Scale bars are 10 µM. B) Quantification of images shown in A. n=20 images/group from 2 independent dissections. Error bars represent SEM. p=0.8264. Abbreviations: C, control; AOD, antioxidant deprivation; SEM, standard error of the mean.

A

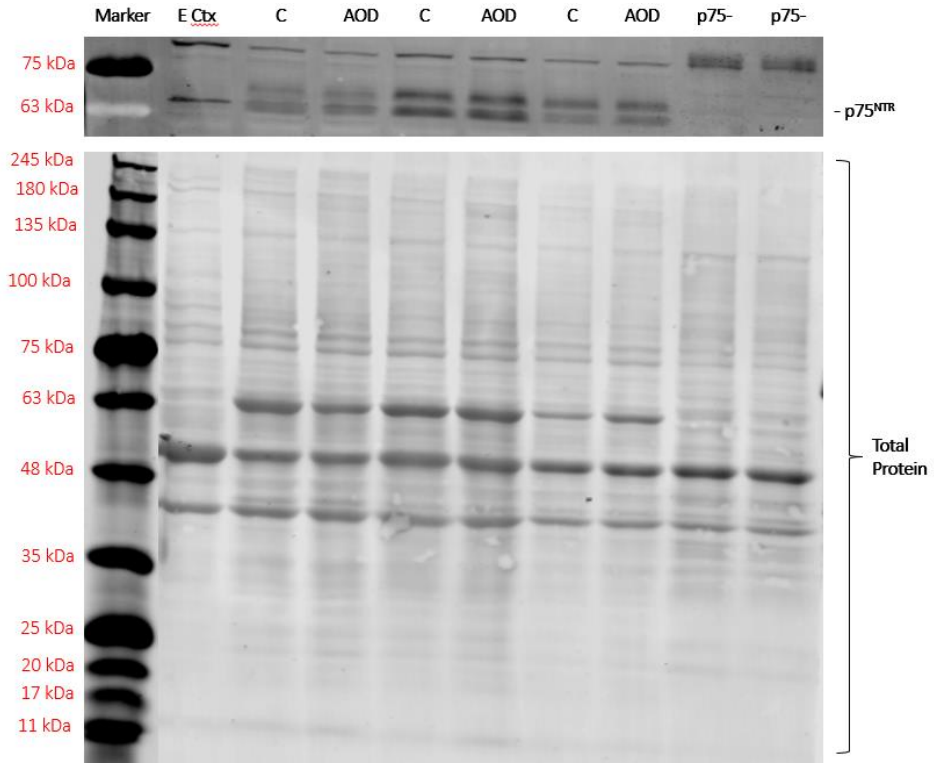
Marker
E Ctx
C
AOD
C
AOD
C
AOD
p75-
p75-
75 kDa
63 kDa
- p75NTR
245 kDa
180 kDa
135 kDa
100 kDa
75 kDa
63 kDa
48 kDa
35 kDa
25 kDa
20 kDa
17 kDa
11 kDa
Total Protein

B

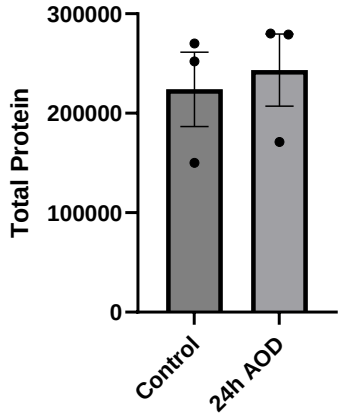
Total Protein
300000
200000
100000
0
Control
24h AOD

C

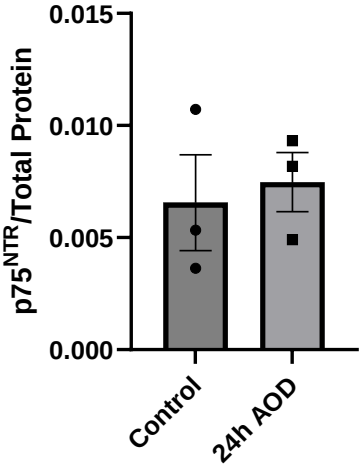
p75NTR/Total Protein
0.015
0.010
0.005
0.000
Control
24h AOD

Figure 8: Oxidative stress has no effect on p75^{NTR} expression in BFCNs in Western blotting.

A) When treated with AOD medium for 24h, there was no difference in full-length p75^{NTR} protein expression compared to control medium. Mouse embryonic cortical tissue was used as a positive control. A cell lysate with p75^{NTR} knockout was used as a negative control. There was no significant difference in total protein loaded between control and AOD cells. B) Quantification of total protein, p=0.4. C) Quantification of full-length p75^{NTR} normalized to total protein, p=0.7342. n=3/group from independent dissections, analyzed in one western blot. Error bars represent SEM. Abbreviations: E Ctx, embryonic cortex; C, control; AOD, antioxidant deprivation; p75-, p75^{NTR} -/-; SEM, standard error of the mean.

4.2.2 Oxidative stress does not affect TrkB levels

For TrkB ICC, it is unknown if the antibody is specific to TrkB.FL only or binds to the truncated isoforms as well, measuring total TrkB. The control group was not normally distributed (W=9142, p=0.0190), whereas the AOD treated group was normally distributed (W=0.9625, p=0.3591), so again the data was analyzed using a Mann-Whitney test. There was no difference in the total TrkB expression measured between control medium and AOD treated groups (Figure 9, p=0.8401).

TrkB.FL, TrkB.T1 + TrkB-Shc, and total TrkB were analyzed separately with western blotting and normalized to total protein. There was a large amount of variance in total protein between samples, which led to there also being large variance in the quantification of TrkB. However, there was no significant difference in total protein loaded between control and 24h AOD groups (Figure 10A,B, p=0.8020). The expected molecular weight of TrkB.FL is 140 kDa, and in the western blot it appeared at 121 kDa. Before normalization TrkB.FL was tested for normality, and control (W=0.7448, p=0.0177) and AOD groups (W=0.7823, p=0.0405) were not normally distributed. They were analyzed using a Mann-Whitney test, and there was no significant difference between groups (Figure 10A,C, p=0.6039). After TrkB.FL was normalized to total protein, based on a Shapiro-Wilk test the control (W=0.7757, p=0.0351) and AOD groups (W=0.7863, p=0.0441) were not normally distributed, so the data was analyzed using a Mann-Whitney test. There was no difference in TrkB.FL expression between control and AOD treated groups (Figure 10A,D, p=0.7381). The expected molecular weight of TrkB.T1 + TrkB-Shc is 90 kDa, and in the western blot it appeared at 89.4 kDa. TrkB.T1 + TrkB-Shc was tested for normality, and it was found that control (W=0.8573, p=0.1801) and AOD groups (W=0.8636, p=0.2017) were normally distributed. According to a t-test, there was no significant difference

between groups (Figure 10A,E, p=8969). When TrkB.T1 + TrkB-Shc was normalized to total protein, control (W=0.8851, p=0.2935) and AOD (W=0.8282, p=0.1038) groups were both normally distributed, so the data were analyzed using an unpaired t-test. There was no significant difference in TrkB.T1+ TrkB-Shc expression between control medium and AOD treated groups (Figure 10A,F, p=0.8995). When combined to account for total TrkB, the control (W=0.8248, p=0.0971) and AOD (W=0.8795, p=0.2667) groups were normally distributed, and there was no significant difference between groups (Figure 10A,G, p=0.9029). After total TrkB was normalized to total protein, a normality test showed that both groups, control (W=0.8906, p=0.3215) and AOD (W=0.8187, p=0.0860), were normally distributed. There was no significant difference in total TrkB levels between control and 24h AOD treated BFCNs (Figure 10,A,H p=0.8808). Power analysis showed that a sample size of 3304 per group would be needed to detect a difference between groups, however the high variance of the data decreases the power of this test. More TrkB.T1 + TrkB-Shc than TrkB.FL was observed in the BFCN cell lysates and adult cortical tissue, whereas embryonic cortical tissue had very little TrkB.T1 + TrkB-Shc, since embryonically mammals mainly express the TrkB.FL isoform. The controls both also express more total TrkB than the samples, likely because they are tissue samples which contain a mixture of cell types in the cortex, rather than pure basal forebrain neuronal cell lysates grown *in vitro*.

A

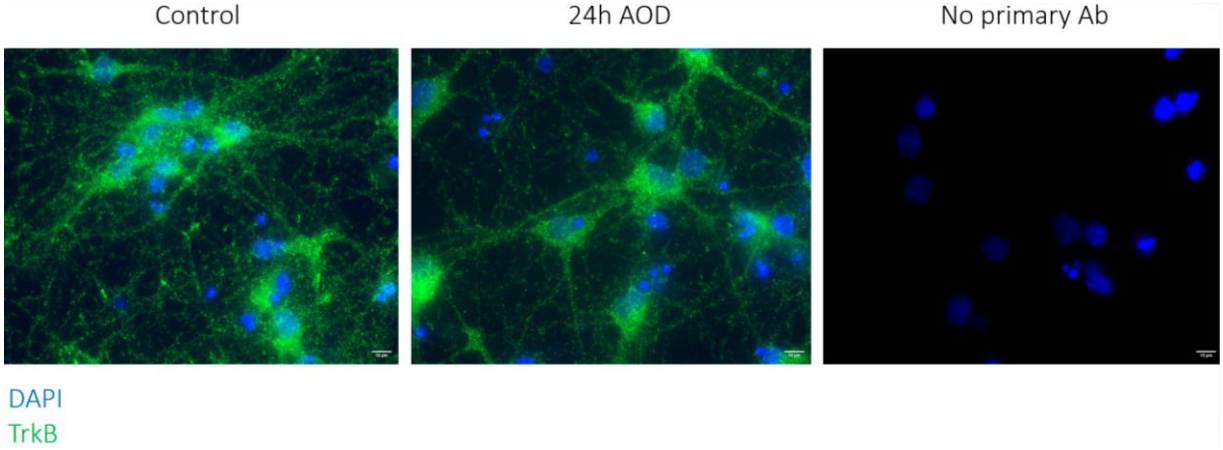

B

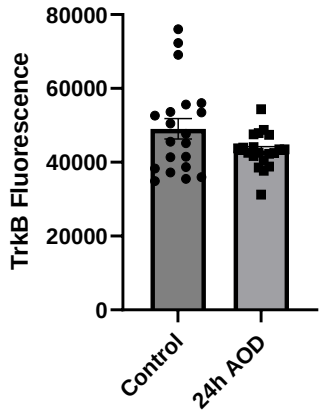

Figure 9: Oxidative stress has no effect on TrkB expression in BFCNs.

A) When treated with AOD medium for 24h, there was no difference in TrkB.FL protein levels compared to control medium shown by ICC. A negative control using no primary antibody showed that there was no non-specific binding, indicating that the fluorescent signal was specific to TrkB. Scale bars are 10 µM. B) Quantification of images shown in A, n=20 images/group, from 2 independent dissections. Error bars represent SEM. p=0.3244. Abbreviations: C, control; AOD, antioxidant deprivation; SEM, standard error of the mean; Ab, antibody.

A

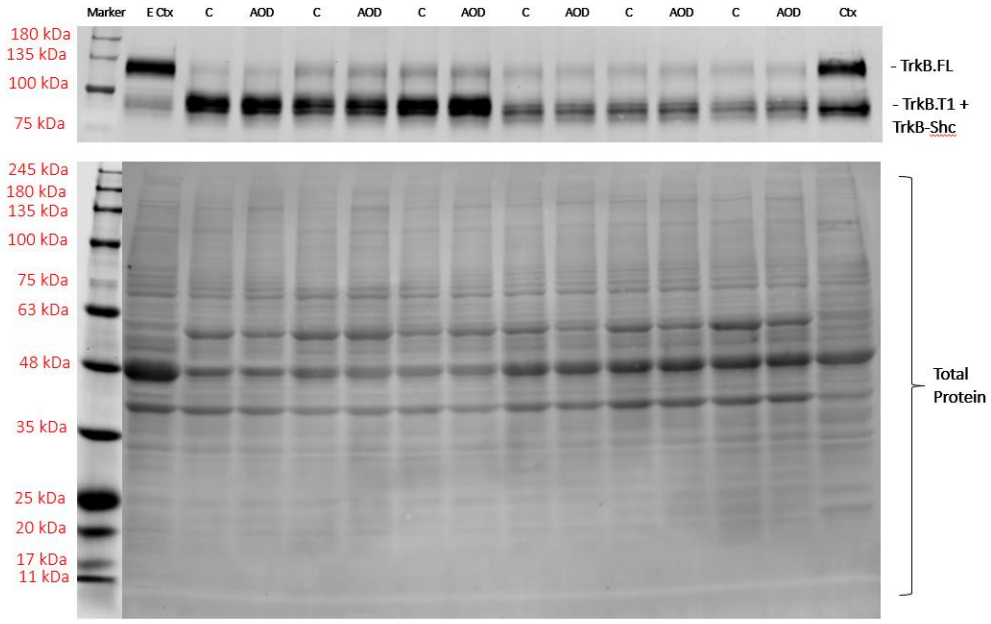
Marker
E Ctx
C
AOD
C
AOD
C
AOD
C
AOD
C
AOD
C
AOD
Ctx
180 kDa
135 kDa
100 kDa
75 kDa
- TrkB.FL
- TrkB.T1 + TrkB-Shc
245 kDa
180 kDa
135 kDa
100 kDa
75 kDa
63 kDa
48 kDa
35 kDa
25 kDa
20 kDa
17 kDa
11 kDa
Total Protein

B

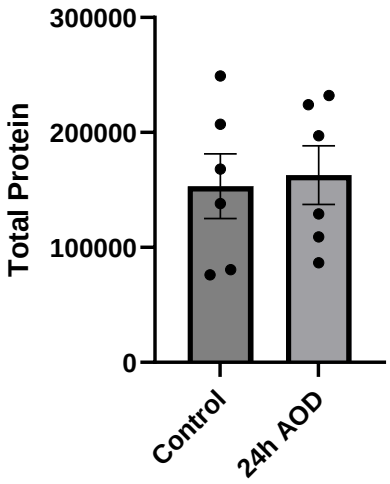
Total Protein
300000
200000
100000
0
Control
24h AOD

C

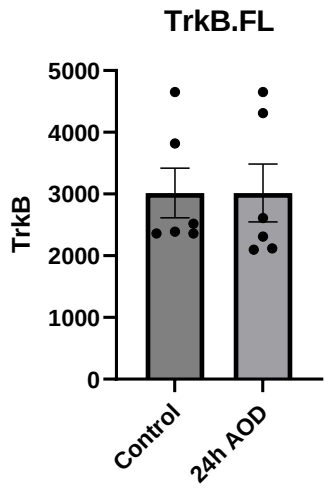
TrkB.FL
TrkB
5000
4000
3000
2000
1000
0
Control
24h AOD

D

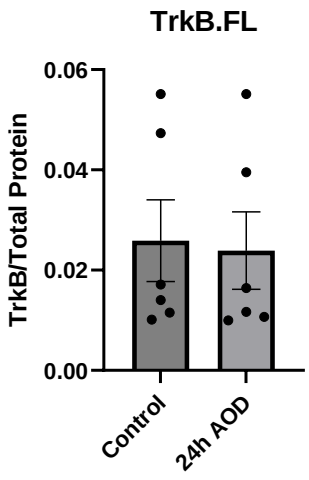
TrkB.FL
TrkB/Total Protein
0.06
0.04
0.02
0.00
Control
24h AOD

E

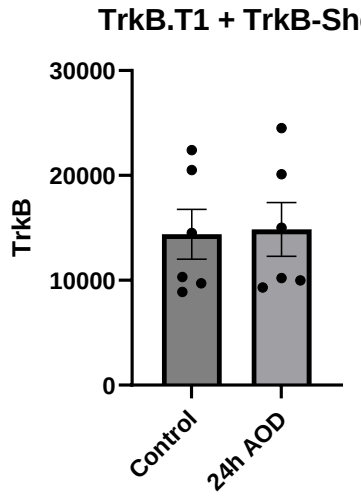
TrkB.T1 + TrkB-Shc
TrkB
30000
20000
10000
0
Control
24h AOD

F

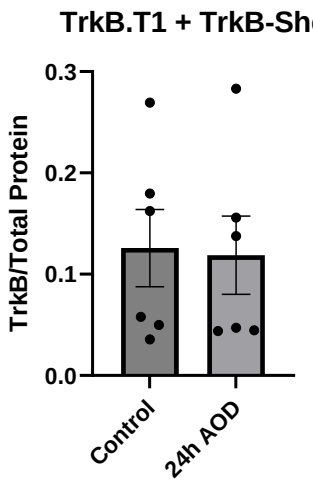
TrkB.T1 + TrkB-Shc
TrkB/Total Protein
0.3
0.2
0.1
0.0
Control
24h AOD

G **H**

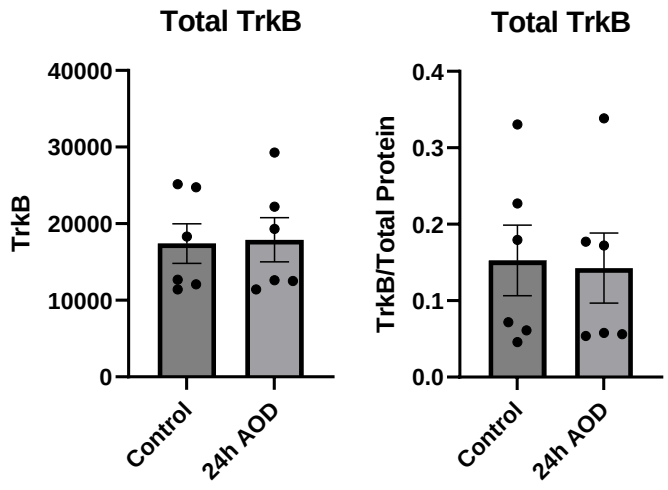

Figure 10: Oxidative stress has no effect on TrkB expression in BFCNs in western blotting. A) TrkB.FL and TrkB.T1 + TrkB-Shc were detected in BFCN cell lysates. When treated with AOD medium for 24h, there was no difference in TrkB.FL, TrkB.T1 + TrkB-Shc, or total TrkB protein expression compared to control medium. Mouse embryonic and adult cortical tissue were used as positive controls. There was no significant difference in total protein loaded between control and AOD cells. B) Quantification of total protein, p=0.8020. C) Quantification of TrkB.FL, p=0.6039. D) Quantification of TrkB.FL/total protein, p=0.7381. E) Quantification of TrkB.T1 + TrkB-Shc, p=0.8969. F) Quantification of TrkB.T1 + TrkB-Shc/total protein, p=0.8995. G) Quantification of total TrkB, p=0.9029. H) Quantification of total TrkB/total protein, p=0.8808. n=6/group from independent dissections, analyzed in one western blot. Error bars represent SEM. Abbreviations: E Ctx, embryonic cortex; Ctx, adult cortex; C, control; AOD, antioxidant deprivation; SEM, standard error of the mean.

4.3 Objective 3

4.3.1 Oxidative stress has no effect on Hook1 levels

Protein expression levels of Hook1 were tested using ICC and western blotting. For ICC, the data was first tested for normality. Based on a Shapiro-Wilk test, both control ($W=0.9327$, $p=0.0581$) and AOD ($W=0.94667$, $p=0.1382$) groups were normally distributed, so, the data was analyzed using an unpaired t-test. No significant difference in Hook1 protein expression was found between control and 24h AOD treated BFCNs (Figure 11, $p=0.4193$).

In western blotting, the Hook1 signal was measured and normalized to total protein. Two separate Hook1 western blots were run. The data from each were combined by normalizing them using their total protein quantification, and a t-test showed that there was no difference in total protein in each blot following normalization ($p=0.6157$). There was a high amount of variance in total protein in the samples, but overall there was no significant difference in total protein loaded between groups (Figure 12A,B, $p=0.7564$). The expected molecular weight of Hook1 is 85 kDa, and the observed molecular weight on the blot was 87 kDa. When Hook1 was normalized to total protein, based on a Shapiro-Wilk test both control ($W=0.9563$, $p=0.7904$) and AOD ($W=0.9410$, $p=0.6675$) groups were normally distributed, so they were compared using an unpaired t-test. There was no significant difference between 24h AOD treated and control groups (Figure 12A,C, $p=0.1835$). Power analysis showed that a samples size of 40 per group would be needed to detect a significant difference between groups.

A

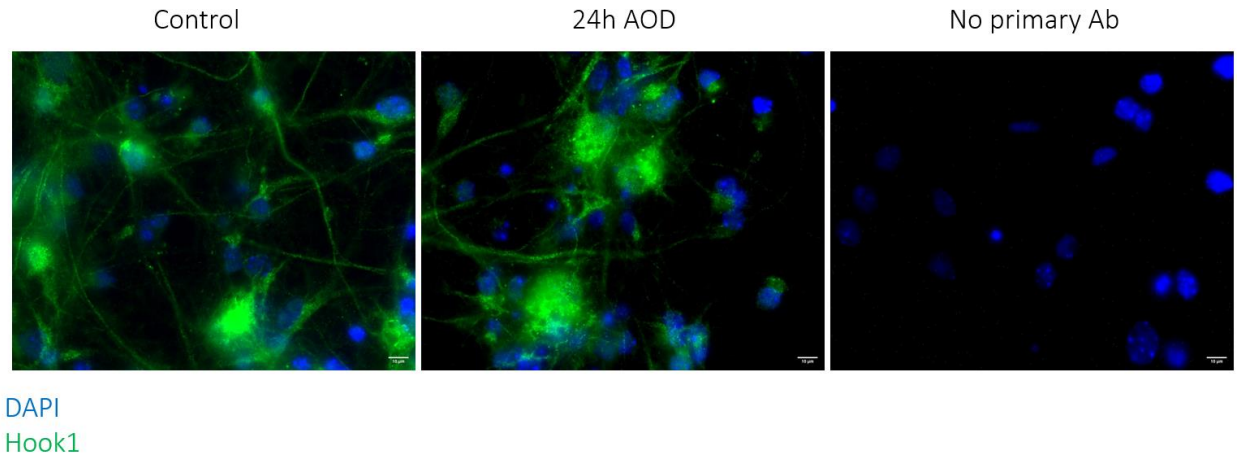

B

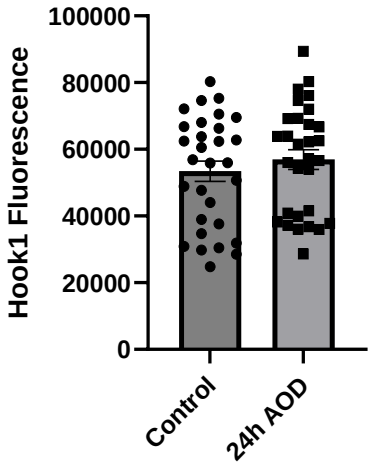

Figure 11: Oxidative stress does not affect Hook1 protein levels.

A) When treated with AOD medium for 24h, there was no difference in Hook1 protein levels compared to control medium shown by ICC. A negative control using no primary antibody showed that there was no non-specific binding, indicating that the fluorescent signal was specific to Hook1. Scale bars are 10 µM. B) Quantification of images shown in A, p=0.4103. n=30 images/group, from 3 independent dissections. Error bars represent SEM. Abbreviations: C, control; AOD, antioxidant deprivation; SEM, standard error of the mean; Ab, antibody.

A

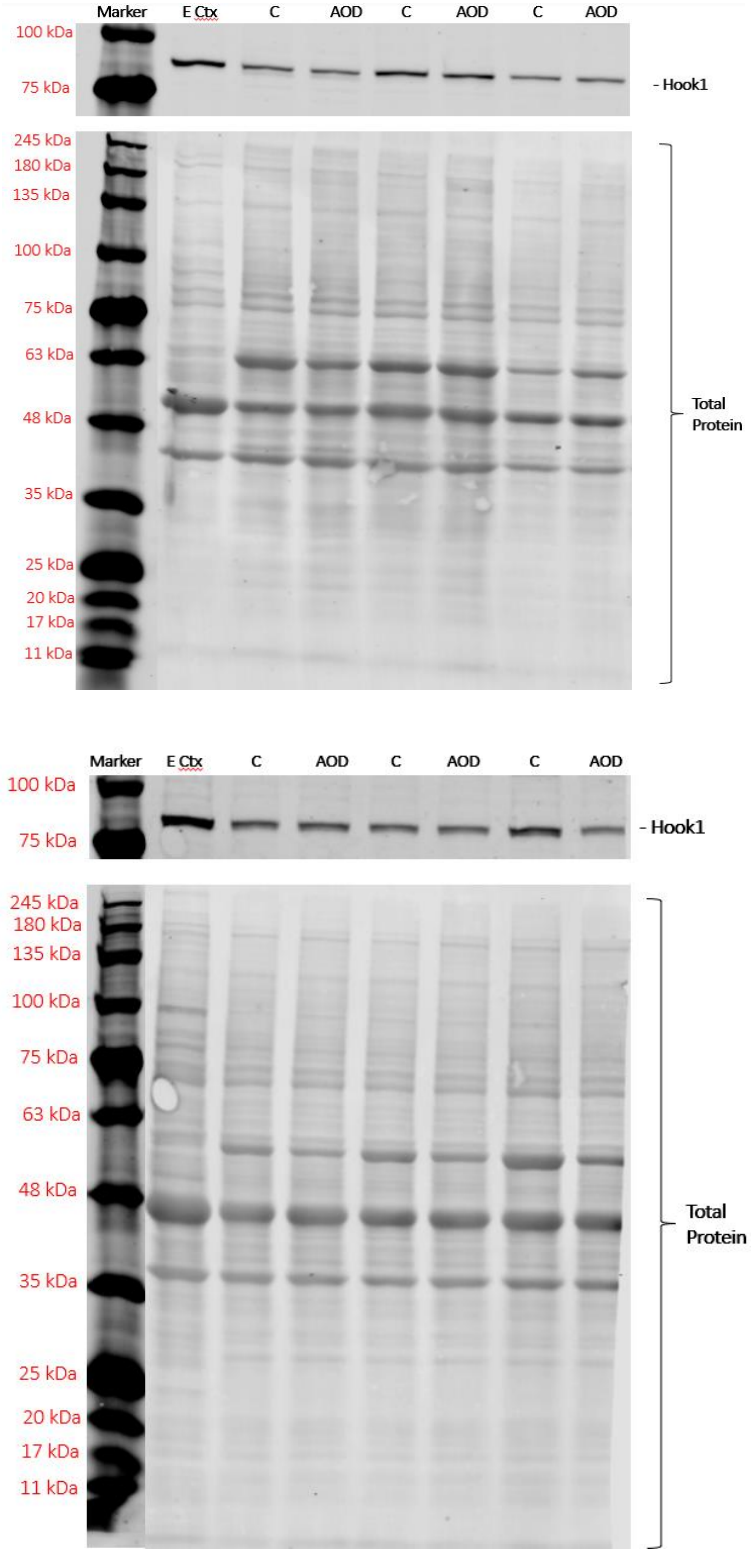
Marker
E Ctx
C
AOD
C
AOD
C
AOD
100 kDa
75 kDa
- Hook1
245 kDa
180 kDa
135 kDa
100 kDa
75 kDa
63 kDa
48 kDa
35 kDa
25 kDa
20 kDa
17 kDa
11 kDa
Total Protein
Marker
E Ctx
C
AOD
C
AOD
C
AOD
100 kDa
75 kDa
- Hook1
245 kDa
180 kDa
135 kDa
100 kDa
75 kDa
63 kDa
48 kDa
35 kDa
25 kDa
20 kDa
17 kDa
11 kDa
Total Protein

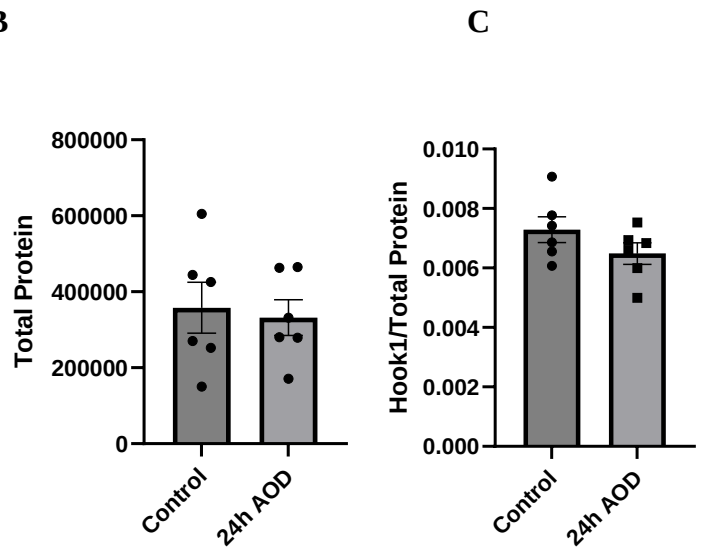

Figure 12: Oxidative stress does not affect Hook1 protein levels in Western blotting.

A) When treated with AOD medium for 24h, there was no difference in Hook1 protein expression compared to control medium. Mouse embryonic cortical tissue was used as a positive control. There was no significant difference in total protein loaded between control and AOD cells. B) Quantification of total protein, p=0.7564. C) Quantification of Hook1 normalized to total protein, p=0.1835. n=6/group from independent dissections, analyzed in two western blots with 3 samples/group on each. Error bars represent SEM. Abbreviations: E Ctx, embryonic cortex; C, control; AOD, antioxidant deprivation; SEM, standard error of the mean.

4.3.2 Oxidative stress has no effect on BICD1 levels

Protein expression levels of BICD1 were tested using ICC and western blotting. For ICC, the data was first tested for normality. Based on a Shapiro-Wilk test, both control (W=0.9273, p=0.1370) and AOD (W=0.8021 p=0.0634) groups were normally distributed, so the data was analyzed using an unpaired t-test. No significant difference in BICD1 protein expression was found between control and 24h AOD treated BFCNs (Figure 13, p=0.0729). Power analysis showed that a sample size of 78 per group would be needed to reach significance. In western blotting, the BICD1 signal was measured and normalized to total protein. First, total protein quantification was done. There were two samples in each group that had a higher amount of total protein than the rest of the samples, but there was no significant difference in total protein loaded between control and 24h AOD treated groups (Figure 14A,B, p=0.8506). The predicted molecular weight of BICD1 is 110 kDa, and the measured molecular weight on the western blot was 116 kDa. When BICD1 was normalized to total protein, only one higher point in the AOD groups was observed, but this was not considered an outlier following the ROUT method. Based on an unpaired t-test there was no significant difference between 24h AOD treated and control groups (Figure 14A,C, p=0.3262). Power analysis showed that a samples size of 75 per group would be needed to detect a significant difference between groups.

A

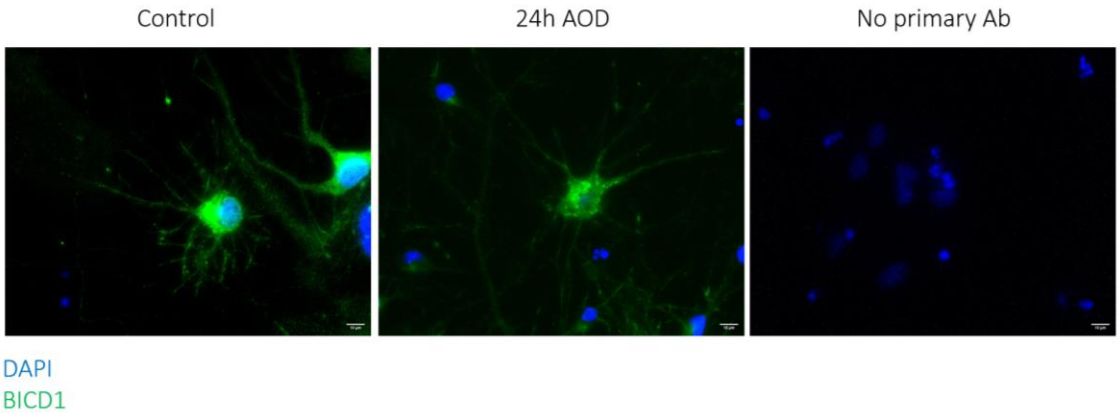

B

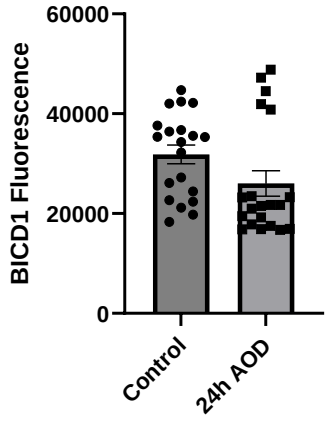

Figure 13: Oxidative stress does not affect BICD1 levels in BFCNs.

A) When treated with AOD medium for 24h, there was no difference in BICD1 protein levels compared to control medium shown by ICC. A negative control using no primary antibody showed that there was no non-specific binding, indicating that the fluorescent signal was specific to BICD1. Scale bars are 10 µM. B) Quantification of images shown in A, p=0.0729. n=30 images/group, from 3 independent dissections. Error bars represent SEM. Abbreviations: C, control; AOD, antioxidant deprivation; SEM, standard error of the mean; Ab, antibody.

A

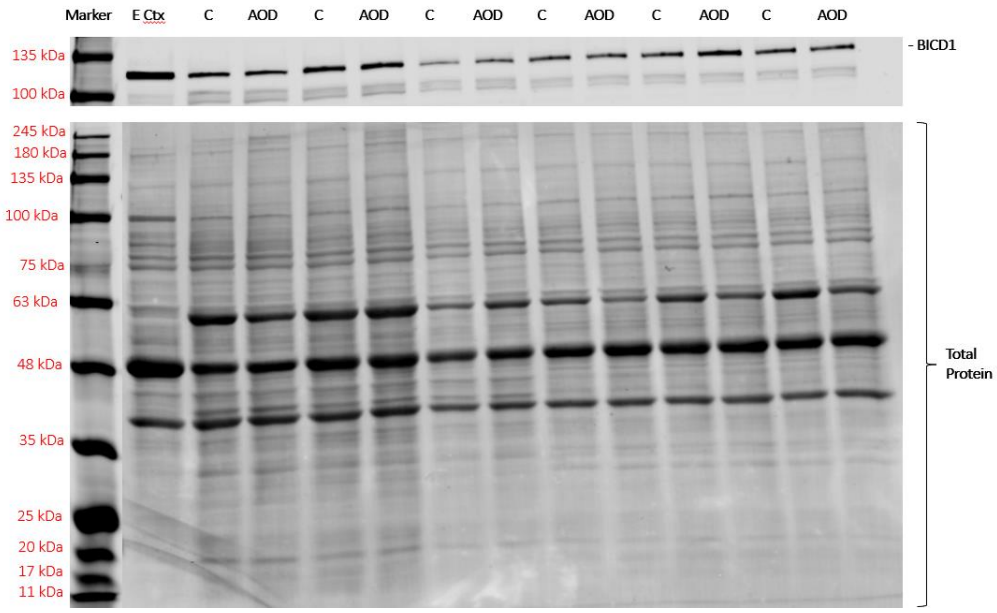
Marker
E Ctx
C
AOD
C
AOD
C
AOD
C
AOD
C
AOD
C
AOD
135 kDa
100 kDa
- BICD1
245 kDa
180 kDa
135 kDa
100 kDa
75 kDa
63 kDa
48 kDa
35 kDa
25 kDa
20 kDa
17 kDa
11 kDa
Total Protein

B

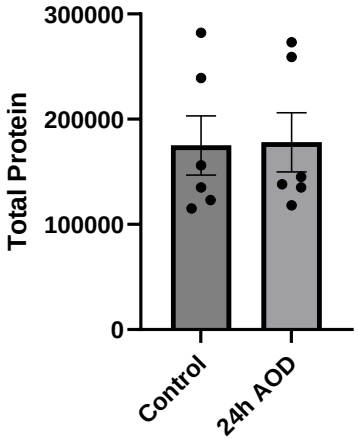
Total Protein
300000
200000
100000
0
Control
24h AOD

C

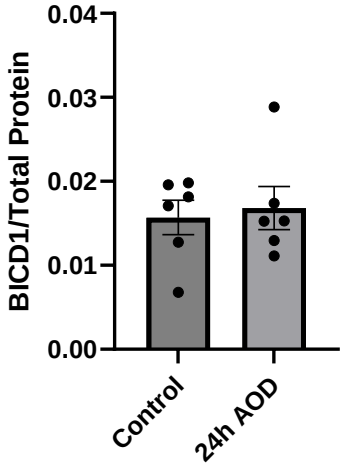
BICD1/Total Protein
0.04
0.03
0.02
0.01
0.00
Control
24h AOD

Figure 14: Oxidative stress does not affect BICD1 protein levels in Western blotting.

A) When treated with AOD medium for 24h, there was no difference in BICD1 protein expression compared to control medium. Mouse embryonic cortical tissue was used as a positive control. There was no significant difference in total protein loaded between control and AOD cells. B) Quantification of total protein, p=0.8506. C) Quantification of BICD1 normalized to total protein, p=0.3262. n=6/group from independent dissections, analyzed in one western blot. Error bars represent SEM. Abbreviations: E Ctx, embryonic cortex; C, control; AOD, antioxidant deprivation; SEM, standard error of the mean.

SECTION 5: DISCUSSION

5.1 Objective 1

I demonstrated that BDNF retrograde axonal transport is decreased in BFCNs with oxidative stress. This was shown using an axonal transport assay, where axons are fluidically isolated from cell bodies so that QD-labelled BDNF can be added to the axon terminals, and BDNF transport can be measured by the accumulation of BDNF at the proximal axons next to the cell body compartment of the chambers. There was significantly reduced BDNF at the proximal axons of BFCNs experiencing oxidative stress compared to control BFCNs, indicating a reduction in retrograde transport. However, there was no significant change in BDNF binding in the axon terminals. There appeared to be a trend towards decreased BDNF binding, but power analysis showed that a very high samples size would be needed to achieve a significant difference in binding between the groups. Overall, these data suggest that BDNF is taken into the axon terminals as normal during oxidative stress, but the transport machinery involved in retrograde transport of BDNF may be impaired.

5.2 Objective 2

Although BDNF axonal binding was not affected by oxidative stress, I expected to see a decrease in TrkB expression, since *in vitro* aging causes reduced BDNF retrograde transport and reduced TrkB expression.[34] I expected no change in $p75^{NTR}$ since it is not known to change in AD or aging, however it was still tested because any change in receptor levels could affect transport and binding of BDNF. Both ICC and western blotting experiments showed that oxidative stress does not affect $p75^{NTR}$ protein expression. The $p75^{NTR}$ western blot had a very low sample size, but it had a high p-value with a large sample size needed to reach significance,

and the ICC results confirmed the results, supporting the hypothesis that $p75^{NTR}$ levels would not change.

It was also found that TrkB receptor protein expression was not affected by oxidative stress. Like most TrkB antibodies, the TrkB antibody used for ICC was produced using the full-length protein and is validated only for binding to TrkB.FL. The exact binding epitope is unknown; therefore, it cannot be determined conclusively whether TrkB expression measured with ICC is representative of just TrkB.FL, or total TrkB including the truncated isoforms. However, western blotting allows the quantification of TrkB.FL and the truncated TrkB isoforms separately, which demonstrates that neither changes with oxidative stress. From the total protein staining on the blot, it is clear that not all lanes had the same total protein loaded. This is due to some samples being quantified using a separate DC protein assay. This was done because the samples from the first three experiments were collected initially and used to test $p75^{NTR}$. Afterwards, more samples were collected and run on another DC assay. Due to variation in the standard preparation, total protein quantification may not be exactly the same between assays. It would have been optimal to quantify all samples on the same DC assay, however there was very little protein available, and all was needed to test the rest of the protein targets, so it was not possible to run the first set of samples again. However, an equal number of control and 24h AOD treated samples were quantified in each DC assay, and there was no significant difference in total protein loaded between groups. When all forms of TrkB were normalized to total protein, there was more variance between the samples than in the non-normalized quantification. So, to better confirm that oxidative stress really has no affect on TrkB levels, it would be best to repeat the experiment with more consistent protein loading. Overall, the data suggest that BDNF retrograde transport deficits caused by oxidative stress may not be due to decreased receptor expression,

which is further supported by the observation that oxidative stress does not affect BDNF binding in BFCNs. A likely alternative is that oxidative stress may lead to alterations in the transport machinery responsible for retrograde endosomal transport. Since there was no change in BDNF binding in axon terminals in the axonal transport assay, it is likely that proteins involved in the regulation of transport along microtubules may be disrupted by oxidative stress.

5.3 Objective 3

I hypothesized that oxidative stress reduces BDNF transport through a decrease in protein expression of the dynein adaptor proteins BICD1 and Hook1. I predicted that this occurred through over-activation of IGF1R by ROS, which increases PI3K/Akt signaling, in turn inhibiting GSK3β through Ser9 phosphorylation, affecting the regulation of gene transcription through TF and histone modifications. However, ICC and western blotting showed that Hook1 protein expression does not change in BFCNs with oxidative stress. BICD1 ICC experiments showed a trend towards decreased expression following oxidative stress. In the AOD group, there is a cluster of data points that are higher than the control group, while most of the other points are lower than the bottom of the SEM of the control group. This may be because the cells were not as healthy in the region of the plate that was imaged, affecting the protein expression quantified. If there are more cells that are dead, then overall protein content will be lower. As well, if the cell density is lower in a certain area from the cell plating, this can affect cell health. However, western blotting confirmed that there was overall no change in BICD1 protein levels. Here, total protein is used to control for any difference in cell density and overall protein production. Similar to the TrkB western blot, the BICD1 blot shows a difference in total protein loaded between the first few samples and the rest. This is for the same reason as previously stated, and again there is no overall difference in protein loaded between control and AOD

groups. When normalized to total protein, control and AOD groups had no difference in BICD1, so oxidative stress does not affect BICD1 expression. I did not have this same issue with the Hook1 western blot because the samples were run on separate gels, and then to combine them I normalized them based on the average total protein loaded.

Although my hypothesis was incorrect, since oxidative stress has no effect on Hook1 or BICD1 levels, it is still unknown whether the IGF1R signaling pathway is affected by oxidative stress in BFCNs. The relationship between IGF1R signaling and oxidative stress is complicated. Although oxidative stress can increase the activation of IGF1R, and reducing IGF1R expression can increase resistance to oxidative stress,[51] it has also been found that oxidative stress can decrease IGF1R expression in certain tissue types such as smooth muscle cells.[70] So, to confirm whether IGF1R signaling is altered by oxidative stress in BFCNs, both expression and activation of IGF1R should be investigated. This could be done using western blotting with antibodies for phospho-IGF1R and total IGF1R to measure activation and total protein levels following oxidative stress. If ROS do increase IGF1R activity, I would expect to see an increase in phospho-IGF1R in BFCNs undergoing oxidative stress. As well, even though BICD1 levels were not changed following oxidative stress, Akt/GSK3β can also phosphorylate BICD1 to stabilize its interaction with dynein, necessary for retrograde transport. So, even though there was no change in BICD1 protein levels, it could be that decreased BICD1/dynein interaction is partly responsible for reduced retrograde transport. This theory could be tested using co-immunoprecipitation of dynein and BICD1 following 24h AOD treatment.

5.4 Future Directions

The next step in this project would be to test other possible mechanisms of transport deficits. There are several other components of the transport machinery and adaptor proteins

involved in regulating retrograde transport of BDNF. One such factor is htt, the protein that is mutated in Huntington's Disease (HD). HD is caused by the mutation of htt, leading to neural degeneration and motor disturbances, but can also cause cognitive deficits.[71] It's been shown that one of the regular functions of htt is the regulation of direction of BDNF vesicle transport in neurons through phosphorylation at Ser421. pSer421-htt promotes anterograde transport by binding to kinesin, while dephosphorylating htt allows retrograde transport by releasing kinesin and allowing interaction with dynein and HAP1.[42] IGF1R signaling through Akt activation phosphorylates htt, while inhibiting htt S421 phosphorylation promotes retrograde BDNF transport in cortical neurons.[42,72] Oxidative stress may increase htt S421 phosphorylation, leading to the decrease in BDNF retrograde transport, either through IGF1R activity or directly by ROS.

Another protein involved in regulating BDNF transport is disrupted in schizophrenia 1 (DISC1). This protein was originally discovered for its involvement in schizophrenia but has since been linked to several disorders that involve oxidative stress.[73] DISC1 decreases with age and is downregulated in AD.[74] DISC1 deficient mice have decreased BDNF in the striatum which is dependent on transport from the cortex, while there is no difference in cortical BDNF levels,[75] and DISC1 mutant mice also have impaired memory.[76] DISC1 is known to form a complex with dynein to associate with the centrosome for transport.[77] It is possible that DISC1 is also decreased by oxidative stress, and this could contribute to impairments in BDNF transport. In the future, this project can focus on DISC1 and htt as possible factors regulating BDNF transport deficits in BFCNs.

5.5 Limitations

A limitation to this study was the equipment used for microscopy. Rather than using BDNF accumulation at proximal axons as a measure of total BDNF transport, it would be ideal

to use time-lapsed images to track BDNF movement.[78] Axonal transport is not a direct linear process, as it often is comprised of heterogeneous motions, including pauses, movement in the anterograde and retrograde direction, and can be dependent on factors such as how proximal or distal to the cell body the axons is. Information such as speed and direction of movement is important for understanding how transport mechanics are affected, however it is lost when measuring protein accumulation rather than directly tracking particle movement. I tried doing this with the EVOS2 FL microscope, however, this is a widefield microscope which produced too much background and not enough image and spatial resolution to accurately track the QD particles. Confocal microscopy is usually used, and has the proper resolution for this function, however, this was not available to me. Due to the location of the microscope, it was not possible to transport the cells to the microscope for live imaging. In the future, it would be best to perform cell culture in the same facility as the confocal microscope so that live tracking can be done. Although I was able to show changes in BDNF transport using quantification of proximal axon BDNF, live tracking would be a better measure of BDNF transport and could provide some insight into the mechanism regulating BDNF transport. Confocal microscopy could also benefit the ICC experiments since it provides better resolution.

Another limitation to this study is the small sample sizes. The basal forebrain is a very small structure, so multiple embryos must be pooled together to get a high enough cell count to plate. To collect protein for western blotting, a much higher number of cells is needed to produce enough protein for quantification. Only a small number of wells could be plated from each dissection, making it impossible to get large sample sizes. It would be best to increase the sample size of experiments, particularly western blots, to reduce the chance of statistical errors.

5.6 Significance

It is well known that neurotrophins such as BDNF play an important role in in the health and synaptic connectivity of neurons, and that they are affected by aging and AD. It has also been established that neurons experience transport deficits in AD, and this contributes to neurodegeneration. However, little research has been done on the role that BDNF transport deficits may have in AD, and how this may occur. Oxidative stress is a state that is implicated in many diseases, and while extensive research has linked oxidative stress to aging and AD, no studies have looked at the impact oxidative stress has on BDNF transport. Currently there is no cure for AD, and the treatment options available only work to slow the progression of symptoms. More work needs to be done to find better ways to treat the underlying causes of AD and prevent the progression of the pathology. To do this, it is important to understand the underlying molecular pathology of both aging and AD. This study aimed to do this by providing insight into the molecular pathology of BDNF transport, showing that oxidative stress negatively impacts BDNF retrograde transport, while ruling out possible mechanisms for this deficit.

REFERENCES

1. Government of Canada, S. C. A portrait of Canada's growing population aged 85 and older from the 2021 Census. https://www12.statcan.gc.ca/census-recensement/2021/as-sa/98-200-X/2021004/98-200-x2021004-eng.cfm (2022).
2. Harada, C. N., Natelson Love, M. C. & Triebel, K. L. Normal Cognitive Aging. *Clin. Geriatr. Med.* **29**, 737–752 (2013).
3. Grothe, M., Heinsen, H. & Teipel, S. J. Atrophy of the Cholinergic Basal Forebrain Over the Adult Age Range and in Early Stages of Alzheimer's Disease. *Biol. Psychiatry* **71**, 805–813 (2012).
4. Dementia numbers in Canada. *Alzheimer Society of Canada* http://alzheimer.ca/en/about-dementia/what-dementia/dementia-numbers-canada.
5. Bondi, M. W., Edmonds, E. C. & Salmon, D. P. Alzheimer's Disease: Past, Present, and Future. *J. Int. Neuropsychol. Soc.* **23**, 818–831 (2017).
6. Benilova, I., Karran, E. & De Strooper, B. The toxic Aβ oligomer and Alzheimer's disease: an emperor in need of clothes. *Nat. Neurosci.* **15**, 349–357 (2012).
7. Chen, G. *et al.* Amyloid beta: structure, biology and structure-based therapeutic development. *Acta Pharmacol. Sin.* **38**, 1205–1235 (2017).
8. Avila, J. *et al.* Tau Structures. *Front. Aging Neurosci.* **8**, 262 (2016).
9. Rankin, C. A. & Gamblin, T. C. Assessing the Toxicity of Tau Aggregation. *J. Alzheimers Dis.* **14**, 411–416 (2008).
10. Lim, S., Haque, Md. M., Kim, D., Kim, D. J. & Kim, Y. K. Cell-based Models To Investigate Tau Aggregation. *Comput. Struct. Biotechnol. J.* **12**, 7–13 (2014).
11. Lasagna-Reeves, C. A. *et al.* Tau oligomers impair memory and induce synaptic and mitochondrial dysfunction in wild-type mice. *Mol. Neurodegener.* **6**, 39 (2011).

12. Patterson, K. R. *et al.* Characterization of Prefibrillar Tau Oligomers in Vitro and in Alzheimer Disease *. *J. Biol. Chem.* **286**, 23063–23076 (2011).

13. Zhao, R.-Z., Jiang, S., Zhang, L. & Yu, Z.-B. Mitochondrial electron transport chain, ROS generation and uncoupling (Review). *Int. J. Mol. Med.* **44**, 3–15 (2019).

14. Turrens, J. F. Mitochondrial formation of reactive oxygen species. *J. Physiol.* **552**, 335–344 (2003).

15. Sharifi-Rad, M. *et al.* Lifestyle, Oxidative Stress, and Antioxidants: Back and Forth in the Pathophysiology of Chronic Diseases. *Front. Physiol.* **11**, (2020).

16. Juan, C. A., Pérez de la Lastra, J. M., Plou, F. J. & Pérez-Lebeña, E. The Chemistry of Reactive Oxygen Species (ROS) Revisited: Outlining Their Role in Biological Macromolecules (DNA, Lipids and Proteins) and Induced Pathologies. *Int. J. Mol. Sci.* **22**, 4642 (2021).

17. Free Radicals in Cross Talk Between Autophagy and Apoptosis. https://www.liebertpub.com/doi/epub/10.1089/ars.2013.5746 doi:10.1089/ars.2013.5746.

18. Kropf, E. & Fahnestock, M. Effects of Reactive Oxygen and Nitrogen Species on TrkA Expression and Signalling: Implications for proNGF in Aging and Alzheimer's Disease. *Cells* **10**, 1983 (2021).

19. Sharifi-Rad, M. *et al.* Impact of Natural Compounds on Neurodegenerative Disorders: From Preclinical to Pharmacotherapeutics. *J. Clin. Med.* **9**, 1061 (2020).

20. Abramov, A. Y., Potapova, E. V., Dremin, V. V. & Dunaev, A. V. Interaction of Oxidative Stress and Misfolded Proteins in the Mechanism of Neurodegeneration. *Life* **10**, 101 (2020).

21. Tchekalarova, J. & Tzoneva, R. Oxidative Stress and Aging as Risk Factors for Alzheimer's Disease and Parkinson's Disease: The Role of the Antioxidant Melatonin. *Int. J. Mol. Sci.* **24**, 3022 (2023).

22. Peng, S., Wuu, J., Mufson, E. J. & Fahnestock, M. Precursor form of brain-derived neurotrophic factor and mature brain-derived neurotrophic factor are decreased in the pre-clinical stages of Alzheimer's disease. *J. Neurochem.* **93**, 1412–1421 (2005).

23. Braschi, C. *et al.* Intranasal delivery of BDNF rescues memory deficits in AD11 mice and reduces brain microgliosis. *Aging Clin. Exp. Res.* **33**, 1223–1238 (2021).

24. Lemmon, M. A. & Schlessinger, J. Cell signaling by receptor-tyrosine kinases. *Cell* **141**, 1117–1134 (2010).

25. Minichiello, L. TrkB signalling pathways in LTP and learning. *Nat. Rev. Neurosci.* **10**, 850–861 (2009).

26. Schirò, G. *et al.* A Brief Overview on BDNF-Trk Pathway in the Nervous System: A Potential Biomarker or Possible Target in Treatment of Multiple Sclerosis? *Front. Neurol.* **13**, 917527 (2022).

27. Kraemer, B. R., Yoon, S. O. & Carter, B. D. The Biological Functions and Signaling Mechanisms of the p75 Neurotrophin Receptor. in *Neurotrophic Factors* (eds. Lewin, G. R. & Carter, B. D.) 121–164 (Springer, 2014). doi:10.1007/978-3-642-45106-5_6.

28. Numakawa, T. & Odaka, H. Brain-Derived Neurotrophic Factor Signaling in the Pathophysiology of Alzheimer's Disease: Beneficial Effects of Flavonoids for Neuroprotection. *Int. J. Mol. Sci.* **22**, 5719 (2021).

29. Basal forebrain degeneration precedes and predicts the cortical spread of Alzheimer's pathology | Nature Communications. https://www.nature.com/articles/ncomms13249.

30. Terry, R. D. *et al.* Physical basis of cognitive alterations in alzheimer's disease: Synapse loss is the major correlate of cognitive impairment. *Ann. Neurol.* **30**, 572–580 (1991).

31. Miranda, M., Morici, J. F., Zanoni, M. B. & Bekinschtein, P. Brain-Derived Neurotrophic Factor: A Key Molecule for Memory in the Healthy and the Pathological Brain. *Front. Cell. Neurosci.* **13**, 363 (2019).

32. Lingor, P., Koch, J. C., Tönges, L. & Bähr, M. Axonal degeneration as a therapeutic target in the CNS. *Cell Tissue Res.* **349**, 289–311 (2012).

33. Kanaan, N. M. *et al.* Axonal degeneration in Alzheimer's disease: When signaling abnormalities meet the axonal transport system. *Exp. Neurol.* **246**, 44–53 (2013).

34. Shekari, A. & Fahnestock, M. Retrograde axonal transport of BDNF and proNGF diminishes with age in basal forebrain cholinergic neurons. *Neurobiol. Aging* **84**, 131–140 (2019).

35. Mattson, M. P. & Pedersen, W. A. Effects of amyloid precursor protein derivatives andoxidative stress on basal forebrain cholinergic systems inALZHEIMERS disease. *Int. J. Dev. Neurosci.* **16**, 737–753 (1998).

36. Lockrow, J. *et al.* Cholinergic degeneration and memory loss delayed by vitamin E in a Down syndrome mouse model. *Exp. Neurol.* **216**, 278–289 (2009).

37. Zheng, J. *et al.* Clathrin-dependent Endocytosis Is Required for TrkB-dependent Akt-mediated Neuronal Protection and Dendritic Growth *. *J. Biol. Chem.* **283**, 13280–13288 (2008).

38. Gibbs, K. L., Greensmith, L. & Schiavo, G. Regulation of Axonal Transport by Protein Kinases. *Trends Biochem. Sci.* **40**, 597–610 (2015).

39. Scaramuzzino, C., Cuoc, E. C., Pla, P., Humbert, S. & Saudou, F. Calcineurin and huntingtin form a calcium-sensing machinery that directs neurotrophic signals to the nucleus. *Sci. Adv.* **8**, eabj8812 (2022).

40. Wu, L. L., Fan, Y., Li, S., Li, X.-J. & Zhou, X.-F. Huntingtin-associated Protein-1 Interacts with Pro-brain-derived Neurotrophic Factor and Mediates Its Transport and Release *. *J. Biol. Chem.* **285**, 5614–5623 (2010).

41. Lim, Y. *et al.* HAP1 Is Required for Endocytosis and Signalling of BDNF and Its Receptors in Neurons. *Mol. Neurobiol.* **55**, 1815–1830 (2018).

42. Colin, E. *et al.* Huntingtin phosphorylation acts as a molecular switch for anterograde/retrograde transport in neurons. *EMBO J.* **27**, 2124–2134 (2008).

43. Chen, X., He, E., Su, C., Zeng, Y. & Xu, J. Huntingtin-associated protein 1-associated intracellular trafficking in neurodegenerative diseases. *Front. Aging Neurosci.* **15**, (2023).

44. He, J., Gong, H. & Luo, Q. BDNF Acutely Modulates Synaptic Transmission and Calcium Signalling in Developing Cortical Neurons. *Cell. Physiol. Biochem.* **16**, 69–76 (2005).

45. Bucci, C., Alifano, P. & Cogli, L. The Role of Rab Proteins in Neuronal Cells and in the Trafficking of Neurotrophin Receptors. *Membranes* **4**, 642–677 (2014).

46. HUTAGALUNG, A. H. & NOVICK, P. J. Role of Rab GTPases in Membrane Traffic and Cell Physiology. *Physiol. Rev.* **91**, 119–149 (2011).

47. LLorens-Martín, M., Torres-Alemán, I. & Trejo, J. L. Reviews: Mechanisms Mediating Brain Plasticity: IGF1 and Adult Hippocampal Neurogenesis. *The Neuroscientist* **15**, 134–148 (2009).

48. Gontier, G., George, C., Chaker, Z., Holzenberger, M. & Aïd, S. Blocking IGF Signaling in Adult Neurons Alleviates Alzheimer's Disease Pathology through Amyloid-β Clearance. *J. Neurosci.* **35**, 11500–11513 (2015).

49. De Magalhaes Filho, C. D. *et al.* Deleting IGF-1 receptor from forebrain neurons confers neuroprotection during stroke and upregulates endocrine somatotropin. *J. Cereb. Blood Flow Metab.* **37**, 396–412 (2017).

50. Annenkov, A. Insulin-Like Growth Factor Receptor Type I (IGF1R) Signaling and Inflammation. in *Encyclopedia of Signaling Molecules* (ed. Choi, S.) 2619–2629 (Springer International Publishing, 2018). doi:10.1007/978-3-319-67199-4_326.

51. Holzenberger, M. *et al.* IGF-1 receptor regulates lifespan and resistance to oxidative stress in mice. *Nature* **421**, 182–187 (2003).

52. Fellows, A. D., Rhymes, E. R., Gibbs, K. L., Greensmith, L. & Schiavo, G. IGF1R regulates retrograde axonal transport of signalling endosomes in motor neurons. *EMBO Rep.* **21**, e49129 (2020).

53. Lalli, G. & Schiavo, G. Analysis of retrograde transport in motor neurons reveals common endocytic carriers for tetanus toxin and neurotrophin receptor p75NTR. *J. Cell Biol.* **156**, 233–240 (2002).

54. Deinhardt, K. *et al.* Rab5 and Rab7 Control Endocytic Sorting along the Axonal Retrograde Transport Pathway. *Neuron* **52**, 293–305 (2006).

55. Terenzio, M. *et al.* Bicaudal-D1 regulates the intracellular sorting and signalling of neurotrophin receptors. *EMBO J.* **33**, 1582–1598 (2014).

56. Wanschers, B. F. J. *et al.* A role for the Rab6B Bicaudal–D1 interaction in retrograde transport in neuronal cells. *Exp. Cell Res.* **313**, 3408–3420 (2007).

57. Cohen, P. & Frame, S. The renaissance of GSK3. *Nat. Rev. Mol. Cell Biol.* **2**, 769–776 (2001).

58. Desbois-Mouthon, C. *et al.* Insulin and IGF-1 stimulate the β-catenin pathway through two signalling cascades involving GSK-3β inhibition and Ras activation. *Oncogene* **20**, 252–259 (2001).

59. Lee, H. J. *et al.* BICD1 mediates HIF1α nuclear translocation in mesenchymal stem cells during hypoxia adaptation. *Cell Death Differ.* **26**, 1716–1734 (2019).

60. Fumoto, K., Hoogenraad, C. C. & Kikuchi, A. GSK-3beta-regulated interaction of BICD with dynein is involved in microtubule anchorage at centrosome. *EMBO J.* **25**, 5670–5682 (2006).

61. Olenick, M. A., Dominguez, R. & Holzbaur, E. L. F. Dynein activator Hook1 is required for trafficking of BDNF-signaling endosomes in neurons. *J. Cell Biol.* **218**, 220–233 (2019).

62. Kitajima, K. *et al.* GSK3β inhibition activates the CDX/HOX pathway and promotes hemogenic endothelial progenitor differentiation from human pluripotent stem cells. *Exp. Hematol.* **44**, 68-74.e10 (2016).

63. Beurel, E., Grieco, S. F. & Jope, R. S. Glycogen synthase kinase-3 (GSK3): regulation, actions, and diseases. *Pharmacol. Ther.* **0**, 114–131 (2015).

64. Herrmann, L. *et al.* Hook Proteins: Association with Alzheimer Pathology and Regulatory Role of Hook3 in Amyloid Beta Generation. *PLOS ONE* **10**, e0119423 (2015).

65. Shekari, A. Ph.D. Thesis – A. Shekari; McMaster University – Neuroscience Graduate Program.

66. Katerji, M., Filippova, M. & Duerksen-Hughes, P. Approaches and Methods to Measure Oxidative Stress in Clinical Samples: Research Applications in the Cancer Field. *Oxid. Med. Cell. Longev.* **2019**, 1279250 (2019).

67. Lançoni, R. *et al.* Validation of the CellRox Deep Red® fluorescent probe to oxidative stress assessment in equine spermatozoa. *Anim. Reprod.* **14**, 437–441 (2017).

68. Home. *Xona Microfluidics* https://xonamicrofluidics.com/.

69. von Schack, D. *et al.* Complete ablation of the neurotrophin receptor p75NTR causes defects both in the nervous and the vascular system. *Nat. Neurosci.* **4**, 977–978 (2001).

70. Kavurma, M. M. *et al.* Oxidative stress regulates IGF1R expression in vascular smooth-muscle cells via p53 and HDAC recruitment. *Biochem. J.* **407**, 79–87 (2007).

71. What is Huntington disease? | Huntington Society of Canada. *Huntington Society of Canada | We Support those facing Huntington Disease* https://www.huntingtonsociety.ca/learn-about-hd/what-is-huntingtons/ (2013).

72. Humbert, S. *et al.* The IGF-1/Akt Pathway Is Neuroprotective in Huntington's Disease and Involves Huntingtin Phosphorylation by Akt. *Dev. Cell* **2**, 831–837 (2002).

73. THOMSON, P. A. *et al.* DISC1 genetics, biology and psychiatric illness. *Front. Biol.* **8**, 1–31 (2013).

74. Lu, J. *et al.* Effects of DISC1 on Alzheimer's disease cell models assessed by iTRAQ proteomics analysis. *Biosci. Rep.* **42**, BSR20211150 (2022).

75. Jaaro-Peled, H. *et al.* The cortico-striatal circuit regulates sensorimotor gating via Disc1/Huntingtin-mediated Bdnf transport. 497446 Preprint at https://doi.org/10.1101/497446 (2018).

76. Park, S. J. *et al.* DISC1 Modulates Neuronal Stress Responses by Gate-Keeping ER-Mitochondria Ca2+ Transfer through the MAM. *Cell Rep.* **21**, 2748–2759 (2017).

77. Kamiya, A. *et al.* A schizophrenia-associated mutation of DISC1 perturbs cerebral cortex development. *Nat. Cell Biol.* **7**, 1167–1178 (2005).

78. Zhao, X. *et al.* Real-time Imaging of Axonal Transport of Quantum Dot-labeled BDNF in Primary Neurons. *JoVE J. Vis. Exp.* e51899 (2014) doi:10.3791/51899.